

Changepoint detection on a graph of time series

Karl L. Hallgren^{1*}, Nicholas A. Heard¹ and Melissa J. Turcotte²

¹Department of Mathematics, Imperial College London

²Microsoft Corporation

Abstract

When analysing multiple time series that may be subject to changepoints, it is sometimes possible to specify a priori, by means of a graph G , which pairs of time series are likely to be impacted by simultaneous changepoints. This article proposes a novel Bayesian changepoint model for multiple time series that borrows strength across clusters of connected time series in G to detect weak signals for synchronous changepoints. The graphical changepoint model is further extended to allow dependence between nearby but not necessarily synchronous changepoints across neighbour time series in G . A novel reversible jump MCMC algorithm making use of auxiliary variables is proposed to sample from the graphical changepoint model. The merit of the proposed model is demonstrated via a changepoint analysis of real network authentication data from Los Alamos National Laboratory (LANL), with some success at detecting weak signals for network intrusions across users that are linked by network connectivity, whilst limiting the number of false alerts.

Keywords: changepoint detection; graphical model; informative prior; auxiliary variable MCMC; cyber-security.

1. Introduction

This article considers the problem of jointly analysing multiple time series that may be subject to changepoints. For each time series, it is of interest to identify the times when the distribution of observations undergoes a change. The focus is on settings for which there are particular clusters of time series more likely to be simultaneously affected by changepoints, where the structure of those clusters is described by a graph.

To motivate our work, we consider an application of changepoint detection in cyber-security. A cyber attack typically changes the behaviour of the target network. Therefore, to detect the presence of a network intrusion, it is informative to monitor for changes in the high-volume data sources that are collected inside an enterprise computer network. However, cyber data are often complex and heterogeneous, and apparent changes are not guaranteed to correspond to an attack. As a result, to limit the number of false alerts and yet not overlook weak signals from genuine, small footprint attacks, it is key to incorporate expert knowledge. A commonly held belief of security experts is that cyber attacks tend to correspond to coordinated sequences of events across multiple connected endpoints on the network (Sexton et al., 2015). For example, some attacks are most likely to be identified through a chain of behavioural changes across related activity types on the same machine, or across machines linked by network connectivity. Hence, there is a requirement for methods that combine evidence from multiple sources to detect changepoints, whilst taking into account which structures of changepoints are *a priori* likely to be of interest.

*Email: karl.hallgren17@imperial.ac.uk

There already exist changepoint detection methods that can borrow strength across multiple time series to detect synchronous changepoints across a subset of the time series; however, limited attention has been given to structures formed by changepoints across multiple time series. For instance, [Jeng et al. \(2012\)](#) uses higher criticism in conjunction with circular binary segmentation to detect synchronous changepoints that affect a proportion of the time series. [Bardwell and Fearnhead \(2017\)](#) gives a Bayesian approach to analysing multiple time series with the aim of detecting regions where the distribution of the data deviates from some normal behaviour, allowing that changepoints may only be present in a subset of time series. [Bolton and Heard \(2018\)](#) presents a Bayesian changepoint model for multivariate processes that are subject to regime switching. [Wang and Samworth \(2018\)](#) proposes a method via projection to study multivariate time series in which, at certain time points, the mean structure changes in a sparse subset of the components. [Grundy et al. \(2020\)](#) presents a method that maps a high-dimensional time series to a two dimensional space in order to detect changes in the mean and variance of the original time series. [Fisch et al. \(2019\)](#) gives an approach to detect collective anomalies within multivariate data streams such that anomalies are not necessarily perfectly aligned. [Bardwell et al. \(2019\)](#) addresses the problem of pooling information across multiple time series to detect the most recent changepoints.

Graphical models provide a useful framework for characterising joint distributions for random variables by means of a graph: the nodes identify the random variables and the edges characterise dependencies among these variables ([Lauritzen, 1996](#)). Areas of application are diverse and include real-life network modelling where edges are natural representations of network connections. In particular, graphical models have been employed to encode prior beliefs on the entities of a graph: for example, in the context of Bayesian variable selection for regression models, [Li and Zhang \(2010\)](#) assumes that covariates lie on an undirected graph and formulates an Ising model prior on the covariate space to incorporate structural information.

This article proposes a novel Bayesian changepoint model for graphs of time series that takes into account structures of changepoints across time series. The model relies on the construction of a class of undirected graphical model-based priors for changepoints that can be used to encode prior beliefs on the dependence structure of changepoints across time series. Our approach assumes that time series indices lie in an undirected graph G that describes which pairs of time series are likely to be simultaneously affected by changepoints. For our purposes, changepoints are represented in discrete time by a binary matrix $S = (S_{i,t})$, such that $S_{i,t}$ indicates whether the time point t is a changepoint for the time series with index i . Then, independent and identical Markov random fields ([Lauritzen, 1996](#)) with respect to G are assumed a priori for the columns of S . As a result, the model assumes that clusters of time series, according to G , are likely to be simultaneously affected by changepoints. A key consequence of the model is that stronger evidence from data is required to infer scattered synchronous changepoints than clustered synchronous changepoints according to G . Furthermore, a more general model is proposed that admits changepoints not occurring at the exact same time to form a priori likely structures across time series; the extended model supposes that changepoints may cluster according to G within some time windows of possibly unknown lengths, which are specific to each series.

A common approach to sampling changepoints for a single time series is that of [Green \(1995\)](#) and consists of using a reversible jump MCMC algorithm to explore the state space of the changepoints: at each iteration of the algorithm, a new changepoint is proposed, or else an existing changepoint is either deleted or shifted to a new position. Specifying a joint model for dependent changepoints across multiple time series introduces additional computational challenges that are not present when changepoints are inferred for each time series independently. It will be demonstrated via a simulation study that it can be impractical to simply propose updates to the changepoints of a randomly chosen time series via one of the moves of [Green \(1995\)](#). To efficiently explore the state space of dependent changepoints, it is necessary to consider joint

proposals for changepoints across multiple time series.

We propose an MCMC algorithm making use of auxiliary variables (Besag and Green, 1993) to sample from the posterior distribution. Swendsen and Wang (1987) and Higdon (1998) provide notable examples of use of auxiliary variables in MCMC schemes that improve mixing and convergence for undirected graphical models. In brief, our sampling strategy is the following. The changepoint parameter space is augmented with auxiliary variables that induce clusters of time series indices according to the dependence graph G . Then, the MCMC algorithm of Green (1995) is extended to sample from the augmented parameter space, such that, at each iteration of the algorithm, a new cluster of changepoints may be proposed or an existing cluster of changepoints may be deleted or shifted.

Bayesian inference for changepoints quantifies uncertainty about the number and the positions of changepoints. However, in some applications such as cyber-security, it will also be necessary to report a point estimate for changepoint parameters. Yet no existing loss function in the literature seems suitable for taking into account both the number and the positions of changepoints. To address this gap, we propose using matchings in graphs (Bondy and Murty, 1976) to define a novel loss function for changepoints, which can be used to obtain a point estimate from a posterior sample of candidate changepoints.

The practical benefits of the proposed graphical model are demonstrated via a changepoint analysis of real network authentication data from Los Alamos National Laboratory (LANL), where a subset of the data relating to a ‘red team’ exercise provide a proxy for intruder behaviour (Kent, 2015). The challenge consists of monitoring for temporal changes in the authentication activity of network users to detect the presence of red team actors. The graphical changepoint model can encode beliefs that signals for network intrusions are a priori likely to occur at nearby times for users historically linked by previous network connectivity. We show that, as a consequence, the proposed model can detect weak signals for red team activity in the network, whilst limiting the number of false alerts, in contrast with a standard model assuming independence of behavioural changes across users.

The remainder of the article is organised as follows. Section 2 presents Bayesian changepoint modelling for multiple time series, proposing a novel loss function for assessing changepoints. Section 3 motivates a graph-dependent changepoint model with an application in cyber-security. Section 4 introduces a class of changepoint models that take into account graph-dependent structures of changepoints across time series. Section 5 proposes an auxiliary variable MCMC sampling strategy. Section 6 presents a simulation study demonstrating the merit of the proposed graphical changepoint model and sampling strategy. Section 7 presents results of a changepoint analysis of network authentication data, illustrating the practical benefits of the proposed model. Section 8 briefly discusses some potential extensions.

2. Changepoint analysis for multiple time series

This section introduces the problem of Bayesian changepoint analysis for multiple time series, proposing a novel loss function for assessing changepoints.

2.1. Model and notation

Suppose we observe L time series of length T . For notational simplicity it will be assumed there are no missing data, but these would present no methodological complication. For all $i = 1, \dots, L$, let $\mathbf{x}_i = (x_{i,1}, \dots, x_{i,T})$ denote the data for the time series with index i , and let $\mathbf{x} = (\mathbf{x}_1, \dots, \mathbf{x}_L)$.

For each time series $i = 1, \dots, L$, suppose there are $k_i \geq 0$ changepoints that partition the passage of time into $k_i + 1$ segments. The ordered locations of the changepoints, denoted by

$\boldsymbol{\tau}_i = (\tau_{i,1}, \dots, \tau_{i,k_i})$, belong to the set \mathcal{T}_{k_i} , where

$$\mathcal{T}_k = \left\{ (\tau_1, \dots, \tau_k) \in \mathbb{N}^k; 1 \equiv \tau_0 < \tau_1 < \dots < \tau_k < \tau_{k+1} \equiv T + 1 \right\}. \quad (1)$$

In parametric modelling, the j th segment for the i th time series, which consists of the time points $\tau_{i,j-1}, \dots, \tau_{i,j}-1$, is assigned a segment parameter $\theta_{i,j}$. The segment parameters for the i th time series are assumed to be independent with identical prior $\pi_i(\theta)$. Conditional on the changepoints and the segment parameters, the data are assumed to be independent and identically distributed such that

$$x_{i,t} \sim f_i(\cdot | \theta_{i,j}), \quad \tau_{i,j-1} \leq t < \tau_{i,j}, \quad (2)$$

for an assumed parametric density $f_i(\cdot | \theta)$ which is not necessarily identical for all time series.

The parameters of interest are the changepoint parameters $(\mathbf{k}, \boldsymbol{\tau})$, where $\mathbf{k} = (k_1, \dots, k_L)$ and $\boldsymbol{\tau} = (\boldsymbol{\tau}_1, \dots, \boldsymbol{\tau}_L)$. Hence, motivated by computational considerations, it is assumed that segment parameters may be marginalised so that the likelihood of the data conditional on the changepoints can be computed. Define

$$\mathcal{L}_i(t_1, t_2) = \int \left(\prod_{t=t_1}^{t_2-1} f_i(x_{i,t} | \theta) \right) \pi_i(\theta) d\theta \quad (3)$$

for all i and $t_1 < t_2$. Then, conditional on the changepoints, the likelihood of the data within the j th segment of the i th time series is $\mathcal{L}_i(\tau_{i,j-1}, \tau_{i,j})$, and the likelihood of the data \mathbf{x} is $\prod_{i=1}^L \prod_{j=1}^{k_i+1} \mathcal{L}_i(\tau_{i,j-1}, \tau_{i,j})$. The integral (3) can be calculated analytically when $\pi_i(\theta)$ is chosen to be conjugate to $f_i(\cdot | \theta)$; and for non-conjugate cases, (3) may be calculated numerically for low-dimensional segment parameters. Given a prior for the changepoint parameters, $\pi(\mathbf{k}, \boldsymbol{\tau})$, one can consequently compute the posterior density function for the changepoint parameters, up to a normalising constant.

When changepoints are assumed to be independent across time series, the posterior distribution of changepoints can be estimated for each time series separately. In this setting, it is standard to assume a priori that, for all time series, discrete time changepoints follow a Bernoulli process (Fearhead, 2006) such that, for all changepoint parameters $(\mathbf{k}, \boldsymbol{\tau})$,

$$\pi(\mathbf{k}, \boldsymbol{\tau} | \mathbf{p}) = \prod_{i=1}^L p_i^{k_i} (1 - p_i)^{T-1-k_i} \quad (4)$$

for some Bernoulli parameters $\mathbf{p} = (p_1, \dots, p_L)$ with $0 < p_i < 1$ for all i . For each time series i , the hyperparameter p_i encodes prior belief on the expected number of changepoints. For notational convenience, we assume that, for all i , $p_i = p$ for some $0 < p < 1$. Note that it will be useful to consider the probability p in terms of the logarithm of the corresponding odds $\text{logit}(p) = \log\{p/(1-p)\}$.

2.2. Estimating changepoint parameters

To give an account of the posterior distribution of changepoint parameters for multiple time series, for each time series i , following Green (1995), one may consider the posterior marginal distribution of the number of changepoints k_i , and the posterior distribution of the changepoint positions $\boldsymbol{\tau}_i$ conditional on k_i . However, in practice, for each time series i , it will also be of interest to report a point estimate $(\hat{k}_i, \hat{\boldsymbol{\tau}}_i)$ for the changepoint parameters $(k_i, \boldsymbol{\tau}_i)$. Following normative Bayesian theory, to define an optimal Bayes estimate for changepoints, we propose a loss function that evaluates the quality of estimated changepoints. When assessing the cost associated with the estimate $(\hat{k}_i, \hat{\boldsymbol{\tau}}_i)$ of $(k_i, \boldsymbol{\tau}_i)$, both the number and the positions of changepoints must be taken into account. To address this challenge, we use matchings in graphs, as defined in Definition 1 and Definition 2, to define a loss function L for changepoint estimates in Definition 3.

Definition 1. (Maximum matching in a graph). Let $B = (V, E)$ be a graph where V is a vertex set and $E \subseteq V \times V$ is an edge set. A matching M in B is a subset of E such that no two edges in M share a common vertex. A maximum matching in B is a matching that is not a subset of a larger matching in B .

Definition 2. (Minimum weight maximum matching in a graph). Let $B = (V, E)$ be a graph with weights $w_{i,j} \geq 0$ for all $(i, j) \in E$. A minimum weight maximum matching in B is a maximum matching in B for which the sum of weights of the edges is minimised.

When B is a weighted bipartite graph, the Kuhn–Munkres algorithm, also known as the Hungarian algorithm, (Bondy and Murty, 1976) finds a minimum weight maximum matching in B ; the time complexity of the algorithm is $\mathcal{O}(|E||V| + |V|^2 \log \log |V|)$, where V and E denote the vertex set and the edge set of B , respectively.

Definition 3. (Loss function L for changepoint estimates). Let $\gamma \geq 0$. For all $k, \hat{k} \geq 0$, $\tau = (\tau_1, \dots, \tau_k) \in \mathcal{T}_k$ and $\hat{\tau} = (\hat{\tau}_1, \dots, \hat{\tau}_{\hat{k}}) \in \mathcal{T}_{\hat{k}}$, let B be the weighted complete bipartite graph with vertex sets $V = \{0, \dots, k\}$ and $\hat{V} = \{0, \dots, \hat{k}\}$, and weights

$$w_{i,j} = \min\{\gamma, |\tau_i - \hat{\tau}_j|\} \quad (5)$$

for all $i \in V$ and $j \in \hat{V}$. Given a minimum weight maximum matching M in B , for all $i \in V$ and $j \in \hat{V}$, let $m_{i,j} = 1$ if i and j are matched, that is $(i, j) \in M$, and $m_{i,j} = 0$ otherwise. Then, define the loss to be

$$L \left[(\hat{k}, \hat{\tau}), (k, \tau) \right] = \gamma |\hat{k} - k| + \frac{1}{2} \sum_{i \in V} \sum_{j \in \hat{V}'} m_{i,j} w_{i,j}. \quad (6)$$

Consider the complete bipartite graph B with independent vertex sets $V = \{0, \dots, k\}$, $\hat{V} = \{0, \dots, \hat{k}\}$ and weights (5). A minimum weight maximum matching M in B gives a matching of the elements of $\hat{\tau}_i$ and τ_i that minimises the sum of distances (5) between matched changepoints. Given M , according to the loss function (6), the cost associated with the estimate $(\hat{k}_i, \hat{\tau}_i)$ of (k_i, τ_i) is then obtained by adding the cost γ for each unmatched changepoint and the total distance between matched changepoints. Note that according to (5), the cost of matching two changepoint positions, that are separated by more than γ time units, is equal to the cost of an unmatched changepoint, namely γ . Therefore, the loss function L takes into account both the number and the positions of changepoints, and the cost γ is chosen to be the maximum acceptable distance between a changepoint position and its estimated position. The optimal Bayes estimate $(\hat{k}_i, \hat{\tau}_i)$ is the changepoint parameters that minimise the expected posterior loss with respect to the posterior marginal distribution of the changepoints (k_i, τ_i) .

Partially as a consequence of the intractability of the normalising constant of the posterior density of changepoint parameters, inference via simulations is required; Section 5 discusses algorithms to obtain a sample of approximate draws from the posterior distribution of changepoints for all time series. Given a sample from the posterior distribution, the optimal Bayes estimate $(\hat{k}_i, \hat{\tau}_i)$ for each series is approximately identified by numerically finding within the sample the changepoint parameters that minimise the estimated posterior expected loss.

3. Motivational example: changepoint detection in cyber-security

To motivate the graphical changepoint model introduced in this article, we consider an application of changepoint detection in cyber-security. A cyber-attack typically changes the behaviour of

connected endpoints on the target network. Therefore, to detect the presence of a network intrusion, it is informative to monitor for changes in the behaviour of network entities.

Kent (2015) presents a comprehensive data set summarising 58 days of traffic on the enterprise network of Los Alamos National Laboratory (LANL), which is available online at <https://csr.lanl.gov/data/cyber1>. The network authentication data consist of records describing authentication activity of users connecting from source computers to destination computers. The occurrence of a ‘red team’ penetration testing operation during the data collection period makes these data suitable for testing network intrusion detection methods. Further details on the data are given in Appendix A.1.

To detect occurrences of malicious activity in the network, the authentication activity of each user is monitored via hourly counts of network logons per source computer. Let M denote the number of distinct source computers in the network. For each user i , let

$$x_{i,t} = (x_{i,t,1}, \dots, x_{i,t,M}), \quad (7)$$

where $x_{i,t,\ell}$ denotes the number of network logons initiated by user i from source computer ℓ during the t -th hour of the 58 day data collection period.

For each user i , it is of interest to detect temporal changes in the distribution of network logons across source computers as possible evidence for malicious activity, and therefore the data $x_{i,1}, \dots, x_{i,T}$ are assumed to follow the changepoint model specified in Section 2.1, with

$$f_i(\cdot | \theta) = f(\cdot | \theta), \quad (8)$$

where $f(\cdot | \theta)$ denotes the density of the multinomial distribution with unknown probability parameter $\theta \sim \text{Dirichlet}(\mathbf{1}^M)$, where $\mathbf{1}^M$ denotes the M dimensional vector of ones, for each time series i . The data exhibit much variability, and some changes can correspond to legitimate activity, but chains of quasi-synchronous changes across multiple users that are connected on the network are a priori more likely to be attack related (Sexton et al., 2015). This follows because attackers must often take control of multiple users to navigate in the network to achieve their objectives.

The network can be represented by a graph

$$G = (V, E), \quad (9)$$

where the set of nodes V denotes the users and an edge $(i, i') \in E \subseteq V \times V$ indicates both user i and user i' successfully initiated a network logon from the same source computer on the same day. The edge set E , which indicates which pairs of users are linked on the network, is assumed to be readily available prior to running network intrusion detection methods; note that, in practice, the edge set could be derived from historic data.

In this setting, the standard prior in (4) is not sufficiently flexible to encode prior beliefs on changepoints. Appendix A.2 exposes limitations resulting from the assumption of changepoint independence across time series through a comparative study. No choice of p seems satisfactory: choosing a small value for p will limit the number of false alerts due to noise and user specific legitimate activity; yet it will also prevent the detection of weak signals for changes shared by different users which are linked in the network, that may be of great interest. It would be preferable to specify a priori that changepoints are more likely to occur simultaneously across time series that are linked in G , in order to require strong evidence from the data for changes impacting a single user, yet possibly weak signals for changes that impact multiple users linked in the network.

This application of changepoint detection in cyber-security provides an example of a setting with multiple time series where it is desirable to specify a priori which pairs of time series are likely to be affected by quasi-synchronous changepoints. For these settings, graphical models provide a framework to describe dependency structures for these pairs of time series.

4. Graphical models for dependent changepoints across multiple time series

This section proposes a flexible class of models for dependent changepoints across time series. Given a graph describing which pairs of time series are a priori likely to be simultaneously affected by changepoints, changepoints are modelled by means of an undirected graphical model. The changepoint model is further extended by relaxing the assumption that dependent changepoints across time series are synchronous; the extended model assumes dependent changepoints across time series correspond to nearby but not necessarily identical time points.

4.1. Synchronous dependent changepoints across time series

4.1.1. Model definition

In Section 2.1, changepoints were most simply defined in terms of changepoint parameters $(\mathbf{k}, \boldsymbol{\tau})$. Subsequently, it will be useful to represent changepoints by means of a binary matrix. For changepoint parameters $(\mathbf{k}, \boldsymbol{\tau})$, let $\mathbf{S} = (S_{i,t})$ be the binary matrix such that, for all $i = 1, \dots, L$ and $t = 2, \dots, T$,

$$S_{i,t} = \begin{cases} 1 & \text{if } \exists j \in \{1, \dots, k_i\} \text{ s.t. } t = \tau_{i,j} \\ 0 & \text{otherwise,} \end{cases} \quad (10)$$

so that $(\mathbf{k}, \boldsymbol{\tau})$ and \mathbf{S} are equivalent representations of the changepoints. Moreover, let $S_{i,0} = S_{i,T+1} = 1$ for all i .

To encode the dependence structure of synchronous changepoints across time series, suppose the time series indices $1, \dots, L$ are the nodes of an undirected graph G with edge set E , and let $\boldsymbol{\lambda} = (\lambda_{i,i'})$ be a symmetric matrix of non-negative edge weights for the graph satisfying $\lambda_{i,i'} > 0$ if and only if $(i, i') \in E$ for all $i, i' = 1, \dots, L$. Then, conditional on $\boldsymbol{\lambda}$, changepoints are assumed to have a prior distribution described by the weighted, undirected graph G such that, for all $(\mathbf{k}, \boldsymbol{\tau})$,

$$\pi(\mathbf{k}, \boldsymbol{\tau} | p, \boldsymbol{\lambda}) = \frac{1}{Z(p, \boldsymbol{\lambda})} \prod_{t=2}^T \exp \left\{ \bar{p} \sum_{i=1}^L S_{i,t} + \sum_{i < i'} \lambda_{i,i'} S_{i,t} S_{i',t} \right\}, \quad (11)$$

for some $0 < p < 1$, where $\bar{p} = \text{logit}(p) = \log\{p/(1-p)\}$ and the normalising constant $Z(p, \boldsymbol{\lambda})$ has no closed form in general. Note that the model in (11) assumes independent and identical Markov random fields (Lauritzen, 1996) for the columns of \mathbf{S} .

If the edge set E is the empty set, implying $\lambda_{i,i'} = 0$ for all i and i' , then the prior distribution in (11) is equivalent to the standard prior for independent changepoints (4); for all changepoint parameters $(\mathbf{k}, \boldsymbol{\tau})$ and for all $0 < p < 1$,

$$\pi(\mathbf{k}, \boldsymbol{\tau} | p, \mathbf{0}) = \pi(\mathbf{k}, \boldsymbol{\tau} | p), \quad (12)$$

where $\mathbf{0}$ is the null matrix and $Z(p, \mathbf{0}) = (1-p)^{-L(T-1)}$.

In general, the prior distribution in (11) takes into account both the number and the relative positions of changepoints across time series; the parameter \bar{p} controls prior belief on the sparsity of changepoints, and the edge weight parameters $\boldsymbol{\lambda}$ control prior belief on the synchronisation of changepoints between time series. For all pairs (i, i') , the larger the edge weight $\lambda_{i,i'} > 0$, the higher the probability for time series i and i' to be simultaneously affected by changepoints. Hence, with the prior in (11) it is possible to specify that changepoints are likely to simultaneously occur across clusters of time series according to G .

To understand how to choose the changepoint hyperparameters \bar{p} and λ in practice, it is instructive to consider the conditional prior distribution of the components of the binary matrix \mathbf{S} . Under (11), the conditional prior distribution of $S_{i,t}$ given $\mathbf{S}_{-(i,t)} = \{S_{i',t'} : (i', t') \neq (i, t)\}$ is

$$\pi(S_{i,t} | \mathbf{S}_{-(i,t)}, p, \lambda) \propto \exp \left\{ S_{i,t} \left(\bar{p} + \sum_{i': (i,i') \in E} \lambda_{i,i'} S_{i',t} \right) \right\}, \quad S_{i,t} \in \{0, 1\}. \quad (13)$$

Therefore, for all i and t , the hyperparameter $p = 1/(1 + \exp\{-\bar{p}\})$ corresponds to the prior probability that t is a changepoint for the i th time series given that no changepoints occur at time t for the graph neighbour time series of i ; and, for all i' such that $(i, i') \in E$, the interaction parameter $\lambda_{i,i'}$ governs how much the conditional prior probability increases if the neighbour time series i' is impacted by a changepoint at time t . Moreover, to perceive the influence of the changepoint hyperparameters on the posterior distribution of changepoints, it is helpful to consider the full conditional distribution of $S_{i,t}$ given $\mathbf{S}_{-(i,t)} = \{S_{i',t'}; (i', t') \neq (i, t)\}$,

$$\begin{aligned} \pi(S_{i,t} | \mathbf{S}_{-(i,t)}, p, \lambda, \mathbf{x}) &\propto \left(\frac{\mathcal{L}_i(\tau'_t, t) \mathcal{L}_i(t, \tau''_t)}{\mathcal{L}_i(\tau'_t, \tau''_t)} \right)^{S_{i,t}} \pi(S_{i,t} | \mathbf{S}_{-(i,t)}, p, \lambda) \\ &\propto \exp \left\{ S_{i,t} \left(\log \left\{ \frac{\mathcal{L}_i(\tau'_t, t) \mathcal{L}_i(t, \tau''_t)}{\mathcal{L}_i(\tau'_t, \tau''_t)} \right\} + \bar{p} + \sum_{i': (i,i') \in E} \lambda_{i,i'} S_{i',t} \right) \right\}, \end{aligned} \quad (14)$$

where \mathcal{L}_i is defined in (3), $\tau'_t = \max\{t' : t' < t, S_{i,t'} = 1\}$ and $\tau''_t = \min\{t' : t' > t, S_{i,t'} = 1\}$. In essence, \bar{p} determines which level of evidence from the data can be considered strong, and the edge weight parameters control how weak signals for synchronous changepoints, relative to \bar{p} , can be combined across time series.

4.1.2. A special case: identical edge weight parameters

In practice, it will often be natural to assume that, for all $(i, i') \in E$, $\lambda_{i,i'} = \lambda$ for some fixed value $\lambda > 0$. For all i and t , let

$$n_{i,t} = \sum_{i': (i,i') \in E} S_{i',t} \quad (15)$$

be the number of neighbour time series of i that are affected by a changepoint at time t . Then, under (11), the conditional prior distribution of $S_{i,t}$ given $\mathbf{S}_{-(i,t)} = \{S_{i',t'} : (i', t') \neq (i, t)\}$ is

$$\pi(S_{i,t} | \mathbf{S}_{-(i,t)}, p, \lambda) \propto \exp \{ S_{i,t} (\bar{p} + \lambda n_{i,t}) \}, \quad S_{i,t} \in \{0, 1\}. \quad (16)$$

Moreover, λ will typically be chosen relative to \bar{p} and the degree distribution of the nodes in G . For example, it can be convenient to assume $\lambda = \lambda_s |\bar{p}| / n$, where n denotes the maximum degree of G , for some $\lambda_s > 0$.

4.2. Examples of graphical dependence structures for changepoints

The prior distribution discussed in Section 4.1 is suitable for a wide variety of settings. This section provides graph motifs that are building blocks to encode the dependence structure of changepoints across multiple time series. For these examples, we consider the parametrisation introduced in Section 4.1.2 and we provide some insight on how to choose the changepoint hyperparameters p and λ , hoping it gives intuition on how to set hyperparameters for more complicated cases. These exemplar dependence structures for changepoints are explored via a simulation study presented in Section 6.

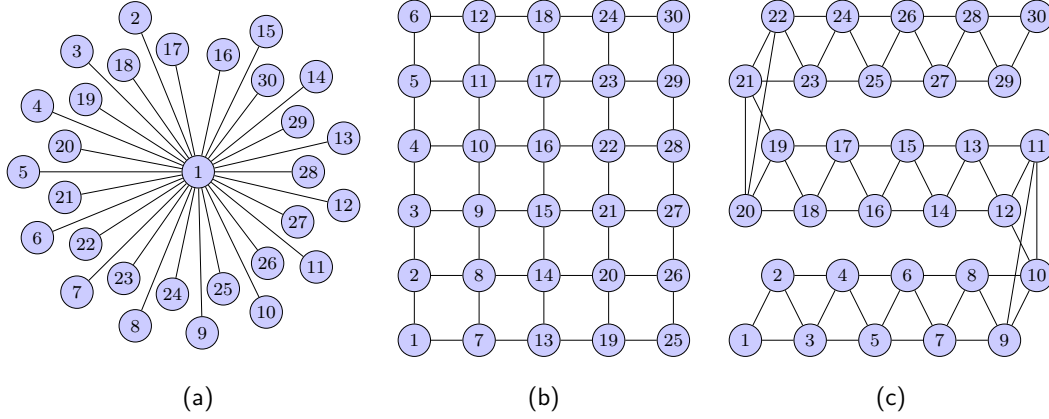


Figure 1: Graphs of time series indices $i \in \{1, \dots, 30\}$ corresponding to different dependence structures for changepoints; panels (a), (b) and (c) correspond to a star, a 6×5 lattice and a 2-chain, respectively.

4.2.1. Stars

Suppose the ultimate goal is to detect changepoints for one particular time series $i = 1$, referred to as the *central* time series, and the remaining time series $i = 2, \dots, L$, which are also susceptible to changepoints, are called the *peripheral* time series. Moreover, for all t , it is known a priori that the central time series is more likely to be affected by a changepoint at time t as the number of peripheral time series affected by a changepoint at time t increases. Furthermore, suppose the peripheral time series changepoints are conditionally independent given the changepoints of the central time series. For the prior for dependent changepoints discussed in Section 4.1, it is then appropriate to consider a star graph for the indices of the time series such that $E = \{(1, 2), \dots, (1, L)\}$. Panel (a) of Figure 1 gives a cartoon representation of a star graph for 30 time series. Under the prior distribution (11), p corresponds to the prior probability that the central time series is affected by a changepoint when no peripheral time series are affected by a changepoint, and $\lambda > 0$ is chosen such that, for all t , the prior conditional probability that t is a changepoint for the central time series is $1/(1 + \exp\{-\bar{p} - n_{1,t}\lambda\})$ where $n_{1,t} \in \{0, \dots, L - 1\}$ is the number of peripheral time series $i > 1$ affected by a changepoint at time t .

4.2.2. Lattices

It might be natural to choose the edge set E to induce a $\ell_1 \times \ell_2$ lattice graph when the number of time series is $L = \ell_1 \ell_2$ for some $\ell_1, \ell_2 > 0$; that is, $(i, i') \in E$ if and only if $|i_1 - i'_1| + |i_2 - i'_2| = 1$ where, for all i , $i - 1 = i_1 \ell_1 + i_2$ with $0 \leq i_2 \leq \ell_2$. Panel (b) of Figure 1 gives a cartoon representation of a 6×5 lattice graph. For example, suppose the data x are recorded for the analysis of some spatio-temporal phenomenon such that $x_{i,t}$ denotes the observation at time t and at the coordinate i of some $\ell_1 \times \ell_2$ grid over a map of the region of interest, and it is of interest to detect the times and the coordinates at which the distribution of the data changes.

With the prior for the dependent changepoints given in (11), one can specify that changepoints are likely to occur as connected clusters of simultaneous changepoints on the lattice. For example, set p to be the prior probability that a changepoint occurs in isolation on the lattice and set $\lambda > 0$ such that, for each i and t , the conditional probability that t is a changepoint for the i th time series is $1/(1 + \exp\{-\bar{p} - n_{i,t}\lambda\})$ where $n_{i,t} \in \{0, \dots, 4\}$ is defined in (15).

4.2.3. r -chains

Another dependence structure of interest arises when there is a natural ordering of the time series, which is encoded by the time series indices $1 < \dots < L$, and changepoints are a priori likely to occur as chains of simultaneous changepoints across consecutive time series. For instance, suppose the data consist of multiple time series that are recorded to monitor various aspects of a system; and, it is of interest to detect some event which evolves through multiple phases, such that each phase is likely to manifest through the perturbation of one aspect of the system. In such a setting, it is appropriate to consider the following graph for the time series indices, which we call an r -chain graph: let $(i, i') \in E$ if and only if $1 \leq |i - i'| \leq r$, for some $r > 0$ chosen to allow gaps of length $r - 1$ within chains of changepoints. Panel (c) of Figure 1 gives a cartoon representation of a 2-chain graph. For the prior given in (11), \bar{p} and λ are chosen such that, for all i and t , the prior conditional probability that t is a changepoint for the i th time series is $1/(1 + \exp\{-\bar{p} - n_{i,t}\lambda\})$ where $n_{i,t} \in \{0, \dots, 2r\}$.

4.3. Extension to asynchronous changepoint dependence

The model in Section 4.1 assumes changepoints are likely to simultaneously affect clusters of time series according to the dependence graph G . In this section, we relax this model to allow dependence between changepoints in different time series at nearby points in time. The extended model relies on representing changepoints as latent changepoints that may be lagged. The latent changepoints are distributed according to the model introduced in Section 4.1 and, conditional on these latent changepoints, time series-specific lags are assumed to be uniformly distributed over some small time window.

Let $(\mathbf{k}, \boldsymbol{\tau})$ be changepoint parameters for multiple time series as defined in Section 2.1, where it is assumed that the i th time series is subject to k_i changepoints whose positions are denoted $\boldsymbol{\tau}_i = (\tau_{i,1}, \dots, \tau_{i,k_i}) \in \mathcal{T}_{k_i}$ as defined in (1). The asynchronous model further assumes that, for all time series $i = 1, \dots, L$, there exist latent changepoint positions $\tilde{\boldsymbol{\tau}} = (\tilde{\boldsymbol{\tau}}_1, \dots, \tilde{\boldsymbol{\tau}}_L)$, $\tilde{\boldsymbol{\tau}}_i = (\tilde{\tau}_{i,1}, \dots, \tilde{\tau}_{i,k_i}) \in \mathcal{T}_{k_i}$, and lags $\mathbf{d} = (\mathbf{d}_1, \dots, \mathbf{d}_L)$, $\mathbf{d}_i = (d_{i,1}, \dots, d_{i,k_i}) \in \{0, \dots, w_i\}^{k_i}$, for $\mathbf{w} = (\mathbf{w}_1, \dots, \mathbf{w}_L)$, where $w_i \geq 0$ is an upper bound for the lags, such that, for all $j = 1, \dots, k_i$, the j th changepoint for time series i is

$$\tau_{i,j} = \tilde{\tau}_{i,j} + d_{i,j}. \quad (17)$$

Let $\tilde{\tau}_{i,0} = \tau_{i,0} = 1$ and $\tilde{\tau}_{i,k_i+1} = \tau_{i,k_i+1} = T + 1$. For all $(k_i, \boldsymbol{\tau}_i)$ and $w_i \geq 0$, if $\tilde{\boldsymbol{\tau}}_i = \boldsymbol{\tau}_i$ and \mathbf{d}_i is the zero vector then (17) holds, and therefore the existence of a corresponding pair $(\tilde{\boldsymbol{\tau}}_i, \mathbf{d}_i)$ is guaranteed. If $w_i = 0$ then the latent changepoints and the changepoints must be identical; yet, in general, given some changepoints $(k_i, \boldsymbol{\tau}_i)$ and $w_i > 0$, there are multiple distinct pairs of latent changepoints $(k_i, \tilde{\boldsymbol{\tau}}_i)$ and lags \mathbf{d}_i satisfying (17).

Suppose the latent changepoints $(\mathbf{k}, \tilde{\boldsymbol{\tau}})$ are distributed according to the prior distribution (11) given some $0 < p < 1$ and graph edge weight parameters $\boldsymbol{\lambda}$. Then, independently for all time series i , conditional on w_i and $(k_i, \tilde{\boldsymbol{\tau}}_i)$, the lags $\mathbf{d}_i = (d_{i,1}, \dots, d_{i,k_i})$ are assumed to be uniformly distributed on the set

$$\mathcal{D}(w_i, k_i, \tilde{\boldsymbol{\tau}}_i) = \left\{ (d_{i,1}, \dots, d_{i,k_i}) \in \{0, \dots, w_i\}^{k_i} : (\tilde{\tau}_{i,1} + d_{i,1}, \dots, \tilde{\tau}_{i,k_i} + d_{i,k_i}) \in \mathcal{T}_{k_i} \right\}, \quad (18)$$

such that, for all $\mathbf{d} = (\mathbf{d}_1, \dots, \mathbf{d}_L)$,

$$\pi(\mathbf{d} | \mathbf{k}, \tilde{\boldsymbol{\tau}}, \mathbf{w}) = \prod_{i=1}^L \frac{\mathbb{1}_{\mathcal{D}(w_i, k_i, \tilde{\boldsymbol{\tau}}_i)}(\mathbf{d}_i)}{|\mathcal{D}(w_i, k_i, \tilde{\boldsymbol{\tau}}_i)|}. \quad (19)$$

Proposition 1 gives a recursion to derive the cardinality of (18).

Proposition 1. (Cardinality of \mathcal{D}). Let $w \geq 0$, $k \geq 0$, $\boldsymbol{\tau} = (\tau_1, \dots, \tau_k) \in \mathcal{T}_k$ with $\tau_0 = 1$ and $\tau_{k+1} = T + 1$, and let $\mathcal{D}(w, k, \boldsymbol{\tau})$ be the set defined in (18).

(i) For all $j \geq 1$ and $l \geq 0$, with $\rho(j, l) = \min\{w + 1, T + 1 - \tau_j\} - (\tau_{j+l} - \tau_j)$, let

$$Q(j, l) = \frac{\Gamma(\rho(j, l) + l + 1)}{\Gamma(\rho(j, l))\Gamma(l + 2)} \mathbb{1}_{\{0, \dots, w\}}(\tau_{j+l} - \tau_j). \quad (20)$$

Moreover, let $Z(0) = 1$, $Z(1) = Q(1, 0)$ and, for all $k > 1$,

$$Z(k) = \sum_{j=1}^k (-1)^{k-j} Z(j-1) Q(j, k-j). \quad (21)$$

Then

$$|\mathcal{D}(w, k, \boldsymbol{\tau})| = Z(k). \quad (22)$$

In particular, if $k = 0$ then $\boldsymbol{\tau}$ is the empty sequence and $\mathcal{D}(w, k, \boldsymbol{\tau})$ contains a unique element, namely the empty sequence.

(ii) $|\mathcal{D}(w, k, \boldsymbol{\tau})| \leq (w + 1)^k$ and the equality holds if and only if $\tau_{j+1} - \tau_j > w$ for all j .

Proof. See Appendix B. □

Consequently, the joint prior density for $(\mathbf{k}, \tilde{\boldsymbol{\tau}}, \mathbf{d})$ is

$$\pi(\mathbf{k}, \tilde{\boldsymbol{\tau}}, \mathbf{d} | p, \boldsymbol{\lambda}, \mathbf{w}) = \frac{\pi(\mathbf{k}, \tilde{\boldsymbol{\tau}} | p, \boldsymbol{\lambda})}{\prod_{i=1}^L |\mathcal{D}(w_i, k_i, \boldsymbol{\tau}_i)|} \quad (23)$$

and the induced changepoint prior distribution for $(\mathbf{k}, \boldsymbol{\tau})$ is

$$\pi(\mathbf{k}, \boldsymbol{\tau} | p, \boldsymbol{\lambda}, \mathbf{w}) = \sum_{(\tilde{\boldsymbol{\tau}}, \mathbf{d}) \in \Upsilon(\mathbf{k}, \boldsymbol{\tau}, \mathbf{w})} \pi(\mathbf{k}, \tilde{\boldsymbol{\tau}}, \mathbf{d} | p, \boldsymbol{\lambda}, \mathbf{w}), \quad (24)$$

where $\Upsilon(\mathbf{k}, \boldsymbol{\tau}, \mathbf{w})$ denotes the set of pairs of latent changepoints and lags, $(\mathbf{k}, \tilde{\boldsymbol{\tau}}, \mathbf{d})$, that identify the changepoints $(\mathbf{k}, \boldsymbol{\tau})$ according to (17). If no lags are allowed, that is $w_i = 0$ for all i , then $\Upsilon(\mathbf{k}, \boldsymbol{\tau}, \mathbf{w}) = \{(\mathbf{k}, \boldsymbol{\tau}, \mathbf{0})\}$ and the prior in (24) is identical to the prior discussed in Section 4.1.

For some applications the upper bounds for the lags, \mathbf{w} , may be known, but this might not be the case. A possible choice of prior distribution for \mathbf{w} would assume that, independently for all time series i , $w_i \sim \text{Geometric}(\eta_i)$ for some series-specific parameter η_i , admitting the possibility the upper bounds for the lags are likely to be larger for some time series than others.

5. Markov chain Monte Carlo inference

Joint sampling of changepoints across time series is required when the assumption of independence for changepoints is relaxed. In this section, we propose a reversible jump MCMC algorithm (Green, 1995) to sample changepoints in multiple time series, $(\mathbf{k}, \boldsymbol{\tau})$. The changepoint parameter space is augmented with auxiliary variables (Besag and Green, 1993; Higdon, 1998) that induce clusters of time series indices according to G . Then, the reversible jump MCMC algorithm of Denison et al. (2002) is extended to sample from the augmented parameter space, thereby providing a means to efficiently explore the changepoint parameter space. At each iteration of the algorithm, a new cluster of changepoints may be proposed or an existing cluster of changepoints may be deleted or shifted. The validity of the proposed MCMC algorithm follows immediately from the reversibility of the proposed moves.

5.1. Sampler for synchronous dependent changepoints

We begin by proposing an MCMC algorithm to sample from the posterior distribution of changepoints when changepoint parameters are a priori distributed according to the prior introduced in Section 4.1, $\pi(\mathbf{k}, \boldsymbol{\tau} | p, \boldsymbol{\lambda})$, given $0 < p < 1$ and some interaction parameters $\boldsymbol{\lambda}$.

To sample changepoints for multiple time series, consider the following adaptation of the standard MCMC algorithm to sample changepoints for a unique time series (Denison et al., 2002), which will be called the “single site updating” MCMC algorithm thereafter. At each iteration of the algorithm, with $(\mathbf{k}, \boldsymbol{\tau})$ denoting the latest particle of the sample chain, propose one of the following two moves: for a uniformly chosen index (i, t) , propose $S_{i,t}$ to be updated to $1 - S_{i,t}$, thereby allowing birth or death of a changepoint; alternatively, the position of a randomly chosen changepoint, $\tau_{i,j}$, is sampled uniformly from $\{\tau_{i,j-1} + 1, \dots, \tau_{i,j+1} - 1\}$.

As a result of the graph interaction parameters $\boldsymbol{\lambda}$, synchronous changepoints can be correlated across time series, and the single site updating MCMC algorithm can become impractical, as illustrated in Section 6.2 within a simulation study. Instead, it will be necessary to propose moves that allow birth, death or shift of clusters of synchronous changepoints according to the graph induced by $\boldsymbol{\lambda}$.

5.1.1. Augmenting the parameter space with auxiliary variables

To provide a means of moving efficiently through the state space of the changepoint parameters, the parameter space is augmented with binary auxiliary variables $\mathbf{u} = (\mathbf{u}_2, \dots, \mathbf{u}_T)$ such that, for all t , \mathbf{u}_t is defined with components $u_t(i, i') \in \{0, 1\}$ for each pair of time series indices $i < i'$. The augmented prior density is assumed to take the conditionally independent form

$$\pi(\mathbf{u} | \boldsymbol{\lambda}, \delta, \mathbf{k}, \boldsymbol{\tau}) = \prod_{t=2}^T \prod_{i < i'} \{1 - q_t(i, i')\}^{u_t(i, i')} q_t(i, i')^{1 - u_t(i, i')}, \quad (25)$$

where

$$q_t(i, i') = \exp\{-\delta \lambda_{i, i'} (1 - |S_{i,t} - S_{i',t} |)\} \quad (26)$$

is the conditional probability that $u_t(i, i') = 0$, given a partial decoupling parameter $\delta \geq 0$ (Higdon, 1998) whose role will be discussed in Section 5.1.2. After observing data \mathbf{x} distributed according to (2), the joint posterior density of the augmented parameters $(\mathbf{k}, \boldsymbol{\tau}, \mathbf{u})$ is

$$\pi(\mathbf{k}, \boldsymbol{\tau}, \mathbf{u} | p, \boldsymbol{\lambda}, \mathbf{x}, \delta) = \pi(\mathbf{u} | \boldsymbol{\lambda}, \delta, \mathbf{k}, \boldsymbol{\tau}) \pi(\mathbf{k}, \boldsymbol{\tau} | p, \boldsymbol{\lambda}, \mathbf{x}). \quad (27)$$

For all t , consider the graph $H_t = (V, E_t)$ with vertex set $V = \{1, \dots, L\}$ and edge set E_t such that $(i, i') \in E_t$ if and only if $u_t(i, i') = 1$ for all $i, i' \in V$. According to (26), if $u_t(i, i') = 1$ then $q_t(i, i') < 1$ and, consequently, $S_{i,t} = S_{i',t}$. As a result, with \mathcal{C}_t denoting the set of connected components of H_t , for all clusters of time series $\gamma \in \mathcal{C}_t$, $S_{i,t} = S_{i',t}$ for all $i, i' \in \gamma$. In other words, the auxiliary variables $\mathbf{u}_t = (u_t(i, i'))$ induce a partition of the time series, \mathcal{C}_t , such that, for each cluster $\gamma \in \mathcal{C}_t$, either all time series or no time series in γ are affected by a changepoint at time t . Moreover, according to (26), if $S_{i,t} = S_{i',t}$ then the conditional probability that $u_t(i, i') = 1$ increases with $\lambda_{i, i'} > 0$, so that clusters induced by \mathbf{u}_t will tend to be clusters on the graph induced by the edge weight parameters.

5.1.2. MCMC algorithm

To generate realisations from the posterior distribution of the changepoints, we consider a “cluster updating” MCMC algorithm that samples from the joint posterior density (27). By inducing

clusters of time series determined by the edge weight parameters for each time point t , the auxiliary variables \mathbf{u} provide a means to efficient exploration of the state space of $(\mathbf{k}, \boldsymbol{\tau})$.

The parameter δ is a tuning parameter for the cluster updating MCMC algorithm. The size of clusters will tend to increase with δ ; in particular, if $\delta = 0$ then, for all t , each cluster corresponds to a unique time series index, even if the edge weights of the dependence graph are large, so that the ‘‘cluster updating’’ MCMC algorithm reduces to the ‘‘single site updating’’ algorithm. Typically δ is fixed (Higdon, 1998) to control the probabilities in (25) and therefore the expected size of clusters. However, we propose to treat $\delta \geq 0$ as an unknown parameter with prior distribution $\pi(\delta)$, so that expected sizes of cluster may vary in the sample; specifically, we assume that $\delta = 0$ with probability δ_0 and that δ is drawn from $\text{Beta}(\delta_1, \delta_2)$ otherwise.

For the cluster updating MCMC algorithm, at each iteration of the algorithm, with $(\mathbf{k}, \boldsymbol{\tau}, \mathbf{u}, \delta)$ denoting the latest particle of the sample chain, one of the following moves is proposed.

Birth/death move

Conditional on the auxiliary variables, the birth/death move proposes the birth or death of a cluster of synchronous changepoints. Sample t' uniformly from $\{2, \dots, T\}$. A cluster γ of time series indices is randomly chosen from $\mathcal{C}_{t'}$, the set of clusters of time series induced by the auxiliary variables $\mathbf{u}_{t'} = (u_{t'}(i, i'))$. Then, leaving the auxiliary variables unchanged, propose changepoint parameters $(\mathbf{k}', \boldsymbol{\tau}')$ such that, for all $i = 1, \dots, L$ and $t = 2, \dots, T$,

$$S'_{i,t} = \begin{cases} 1 - S_{i,t} & \text{if } i \in \gamma \text{ and } t = t' \\ S_{i,t} & \text{otherwise,} \end{cases} \quad (28)$$

where S and S' are binary matrix representations of $(\mathbf{k}, \boldsymbol{\tau})$ and $(\mathbf{k}', \boldsymbol{\tau}')$ according to (10), respectively.

Shift move

The shift move proposes to shift the position of a cluster of synchronous changepoints. First, a time unit t is uniformly chosen from $\{t : \sum_{i=1}^L S_{i,t} > 0\}$. Let $\mathcal{C}_t^* \subseteq \mathcal{C}_t$ denote the set of clusters of time series indices γ induced by \mathbf{u}_t such that, for all $i \in \gamma$, $S_{i,t} = 1$. A cluster γ is uniformly chosen from \mathcal{C}_t^* . For all $i \in \gamma$, let j_i be the index of the changepoint with position t for the i th time series, that is $\tau_{i,j_i} = t$. Then, sample uniformly t' from $\bigcap_{i \in \gamma} \{\tau_{i,j_i-1} + 1, \dots, \tau_{i,j_i+1} - 1\}$ and propose changepoint parameters $(\mathbf{k}, \boldsymbol{\tau}')$ that are identical to $(\mathbf{k}, \boldsymbol{\tau})$ but with $\tau'_{i,j_i} = t'$, for all $i \in \gamma$.

In parallel, it is required to propose auxiliary variables \mathbf{u}' which are adapted to $(\mathbf{k}, \boldsymbol{\tau}')$. The updated auxiliary variables differ from \mathbf{u} as follows. For all $i, i' \in \gamma$, $u'_{t'}(i, i') = u_t(i, i')$ and $u'_t(i, i') = u_{t'}(i, i')$; for all $i \in \gamma$ and $i' \notin \gamma$ such that $t' \notin \boldsymbol{\tau}_{i'}$, $u'_{t'}(i, i') = 0$; and, ensuring reversibility of the move, for all $i \in \gamma$ and $i' \notin \gamma$ such that $t \notin \boldsymbol{\tau}_{i'}$, $u'_t(i, i')$ is sampled conditionally on $(\mathbf{k}, \boldsymbol{\tau}')$ according to the Bernoulli $(1 - \exp\{-\delta \lambda_{i,i'}(1 - |S_{i,t} - S'_{i,t}|\})$ target distribution implied by (25).

Update of auxiliary variables

Changepoints are left unchanged, δ is sampled from its prior distribution, and auxiliary variables are sampled from the full conditional distribution given in (25), thereby proposing an updated clustering of time series indices for all t .

5.2. Sampler for asynchronous dependent changepoints

According to the changepoint model (24) introduced in Section 4.3, changepoints do not need to occur at the same time to be related. Consequently, to explore the changepoint parameter space it

will be required to propose the birth, death or shift of clusters of asynchronous changepoints. This section extends the MCMC algorithm from Section 5.1 to sample from the posterior distribution of changepoints when changepoint parameters are a priori distributed according to $\pi(\mathbf{k}, \boldsymbol{\tau} | p, \boldsymbol{\lambda}, \mathbf{w})$ from (24).

Recall that under the asynchronous model, changepoints $(\mathbf{k}, \boldsymbol{\tau})$ are deterministically specified by latent changepoints $(\mathbf{k}, \tilde{\boldsymbol{\tau}})$ and unknown lags \mathbf{d} according to (17). Therefore, a sample from $(\mathbf{k}, \boldsymbol{\tau})$ can be obtained from a sample from $(\mathbf{k}, \tilde{\boldsymbol{\tau}}, \mathbf{d})$. Next, we propose a sampler from the joint posterior distribution of $(\mathbf{k}, \tilde{\boldsymbol{\tau}}, \mathbf{d})$, updated from the prior density (23) by the observed data \mathbf{x} , thereby providing a means to obtain a sample from the posterior distribution of $(\mathbf{k}, \boldsymbol{\tau})$.

As in Section 5.1, the parameter space is augmented with auxiliary variables $\mathbf{u} = (\mathbf{u}_2, \dots, \mathbf{u}_T)$ to facilitate the exploration of the state space of the parameters of interest $(\mathbf{k}, \tilde{\boldsymbol{\tau}}, \mathbf{d})$. Conditionally on latent changepoints $(\mathbf{k}, \tilde{\boldsymbol{\tau}})$ and independently of the lags and the data, for all t and $i < i'$, $u_t(i, i')$ is assumed to be distributed according to (25), such that $u_t(i, i') \sim \text{Bernoulli}\left(1 - \exp\{-\delta \lambda_{i, i'}(1 - |\tilde{S}_{i, t} - \tilde{S}_{i', t}|\})\right)$, where \tilde{S} is the binary matrix representation of $(\mathbf{k}, \tilde{\boldsymbol{\tau}})$ according to (10). As described in Section 5.1.1, it follows that the auxiliary variables $\mathbf{u}_t = (u_t(i, i'))$ induce a partition of the time series, \mathcal{C}_t , such that, for each cluster $\gamma \in \mathcal{C}_t$, either all time series or no time series in γ are affected by a latent changepoint at time t .

The joint posterior density of the augmented parameters $(\mathbf{k}, \tilde{\boldsymbol{\tau}}, \mathbf{d}, \mathbf{u})$ is

$$\pi(\mathbf{k}, \tilde{\boldsymbol{\tau}}, \mathbf{d}, \mathbf{u} | p, \boldsymbol{\lambda}, \mathbf{w}, \mathbf{x}, \delta) = \pi(\mathbf{u} | \boldsymbol{\lambda}, \delta, \mathbf{k}, \tilde{\boldsymbol{\tau}}) \pi(\mathbf{k}, \tilde{\boldsymbol{\tau}}, \mathbf{d} | p, \boldsymbol{\lambda}, \mathbf{w}, \mathbf{x}). \quad (29)$$

To sample from the posterior distribution of $(\mathbf{k}, \tilde{\boldsymbol{\tau}}, \mathbf{d}, \mathbf{u})$, or $(\mathbf{k}, \tilde{\boldsymbol{\tau}}, \mathbf{d}, \mathbf{u}, \mathbf{w})$ if upper bounds for the lags are a priori unknown, the MCMC algorithm discussed in Section 5.1 is extended as follows: the birth/death and shift moves are adapted to pairs of latent changepoints and lags; and additional moves are introduced for updating the lags. For the lags, note that according to (18), for all $i = 1, \dots, L$ and $j = 1, \dots, k_i$, to maintain monotonicity in the changepoints, the lag associated to the j th changepoint of the i th time series must satisfy

$$d_{i, j} \in \mathcal{D}_j(w_i, k_i, \tilde{\boldsymbol{\tau}}_i) = \{\ell \in \mathbb{N}; d_- \leq \ell \leq d^+\}, \quad (30)$$

where $d_- = \max(0, d_{i, j-1} + \tau_{i, j-1} - \tau_{i, j} + 1)$ and $d^+ = \min(w_i, d_{i, j+1} + \tau_{i, j+1} - \tau_{i, j} - 1)$; and the full conditional probability distribution of $d_{i, j}$ is such that, for all $d_{i, j} \in \mathcal{D}_j(w_i, k_i, \tilde{\boldsymbol{\tau}}_i)$,

$$\pi(d_{i, j} | \mathbf{d}_{-(i, j)}, k_i, \tilde{\boldsymbol{\tau}}_i, w_i, \mathbf{x}_i) \propto \mathcal{L}_i(\tilde{\tau}_{i, j-1} + d_{i, j-1}, \tilde{\tau}_{i, j} + d_{i, j}) \mathcal{L}_i(\tilde{\tau}_{i, j} + d_{i, j}, \tilde{\tau}_{i, j+1} + d_{i, j+1}) \quad (31)$$

where $\mathbf{d}_{-(i, j)} = \{d_{i', j'}; (i', j') \neq (i, j)\}$ and \mathcal{L}_i is defined in (3).

For the extended cluster updating MCMC algorithm, at each iteration of the algorithm, with $(\mathbf{k}, \tilde{\boldsymbol{\tau}}, \mathbf{d}, \mathbf{u}, \mathbf{w})$ denoting the latest particle of the sample chain, one of the following moves is proposed.

Extended birth/death move

The extended birth/death move proposes the birth or death of a cluster of asynchronous changepoints. First, conditionally on the auxiliary variables, latent changepoints $(\mathbf{k}', \tilde{\boldsymbol{\tau}}')$ are proposed according to the birth/death move detailed in Section 5.1: for all time series $i \in \gamma \subseteq \{1, \dots, L\}$, the birth or death of latent changepoint with position t is proposed. Then, updated lags are proposed conditional on $(\mathbf{k}', \tilde{\boldsymbol{\tau}}')$: If the birth of changepoints is proposed, then, for all time series $i \in \gamma$, there is j_i such that $\tilde{\tau}'_{i, j_i} = t$, and the lags $\mathbf{d}'_i = (d_{i, 1}, \dots, d_{i, j_i-1}, d'_{i, j_i}, d_{i, j_i+1}, \dots, d_{i, k_i})$ are proposed for the i th time series, where d'_{i, j_i} is sampled from the full conditional distribution (31); otherwise, if the death of changepoints is proposed, then, for all $i \in \gamma$, there is j_i such that $\tilde{\tau}_{i, j_i} = t$, and the lags $\mathbf{d}'_i = (d_{i, 1}, \dots, d_{i, j_i-1}, d_{i, j_i+1}, \dots, d_{i, k_i})$ are proposed for the i th time series.

Extended shift move

The extended shift move proposes to shift the positions of a cluster of asynchronous changepoints. First, latent changepoints $(\mathbf{k}', \tilde{\boldsymbol{\tau}}')$ and auxiliary variables \mathbf{u}' are proposed according to the shift move discussed in Section 5.1: for all time series with index $i \in \gamma$, the position t' is proposed for latent changepoint with position t . Then, for all $i \in \gamma$, letting j_i denote the index such that $\tilde{\tau}'_{i,j_i} = t'$, propose d'_{i,j_i} from the full conditional distribution (31).

Update of auxiliary variables

δ is sampled from its prior distribution and, conditional on latent changepoints $(\mathbf{k}, \tilde{\boldsymbol{\tau}})$, auxiliary variables are sampled from their full conditional distribution (25).

Update of lags

A pair (i, j) is uniformly chosen from $\{(i, j); i = 1, \dots, L \text{ and } j = 1, \dots, k_i\}$, and the lag $d_{i,j}$ is sampled from the full conditional distribution given in (31).

Update of upper bounds for lags

If the maximal lags \mathbf{w} are a priori unknown, for a randomly chosen time series with index i it is proposed to update w_i to $w'_i = w_i + \sigma$ with probability $1/2$, and to update w_i to $w'_i = |w_i - \sigma|$ otherwise, where σ is drawn from $\text{Geometric}(\rho)$ for some $0 < \rho < 1$. Proposing to update w_i requires proposing updated lags $\mathbf{d}'_i = (d'_{i,1}, \dots, d'_{i,k_i}) \in \mathcal{D}(w'_i, k_i, \tilde{\boldsymbol{\tau}}_i)$ for the i th time series. For $j = 1, \dots, k_i$, given w'_i and $(d'_{i,1}, \dots, d'_{i,j-1}, d_{i,j+1}, \dots, d_{i,k_i})$, the lag $d'_{i,j}$ is sampled from the full conditional distribution (31).

5.3. Time complexity and initialisation of the sampler

Specifying that changepoints are dependent across time series necessitates joint sampling of changepoint parameters $(\mathbf{k}, \boldsymbol{\tau})$, what will require a greater running time than sampling independent changepoint parameters $(k_i, \boldsymbol{\tau}_i)$ for each time series i in parallel. In particular, the running time of the proposed sampler will tend to increase with the number of edges $|E|$ in the graph G describing which pairs of time series are a priori likely to be impacted by simultaneous changepoints.

To speed-up the convergence of the sampler, we may consider the following initialisation of the sample chain: latent changepoints are set to be the Bayes changepoint estimates, according the loss function defined in Definition 3, that correspond to the standard model assuming independent changepoints across time series with prior $\pi(\mathbf{k}, \boldsymbol{\tau} | \mathbf{p})$, and that are obtained in parallel for each time series i ; initial lags, upper bounds for lags and auxiliary variables are set to 0. As a result, the burn-in for the sampler begins with a sensible positioning of changepoints at a limited cost: no iterations for the burn-in of the joint sampling of changepoints across time series are wasted identifying strong signals for changepoints, relative to \bar{p} .

6. Simulation study

A simulation study is presented to demonstrate the model for dependent changepoints proposed in Section 4 and the sampling strategy discussed in Section 5. In particular, the graphical changepoint model is compared with the standard model for independent changepoints, which assumes all edge weight parameters are null (12).

Consider $L = 30$ time series each of length $T = 300$, which are assumed to follow the changepoint model discussed in Section 2.1, with $f_i(\cdot | \theta)$ corresponding to $\text{Poisson}(\theta)$ and $\theta \sim$

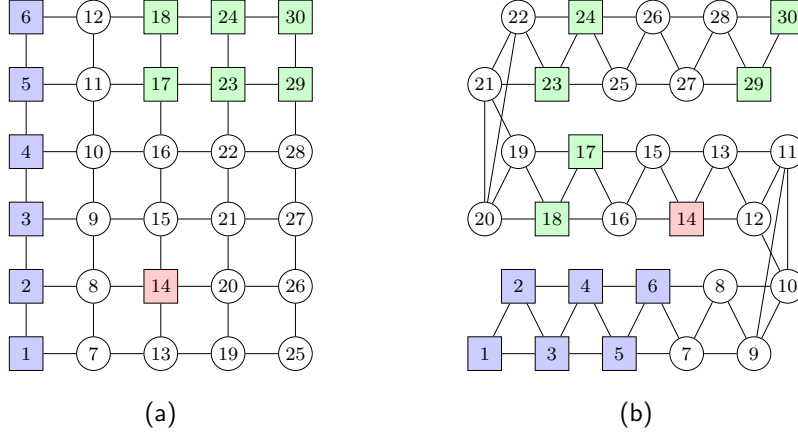


Figure 2: Graphs of time series indices $i \in \{1, \dots, 30\}$ representing different dependence structures of changepoints discussed in Section 4.2; panels (a) and (b) correspond to a 6×5 lattice and a 2-chain, respectively. For all i , circles indicate $i \in N$ and squares indicate $i \in C$; colours blue, green and red indicate that $i \in C_1$, C_2 and C_3 , respectively.

$\Gamma(100, 0.1)$ for each time series i . To sample data for the simulation study, the set of time series indices $\{1, \dots, L\}$ is partitioned into two sets C and $N = \{1, \dots, L\} \setminus C$ such that $k_i = 1$ if $i \in C$ and $k_i = 0$ if $i \in N$, so that each time series is either impacted by a single changepoint or not impacted by changepoints. In the following experiments, different graphical models of dependence structures of changepoints across time series are considered by means of further divisions of the set C into subsets C_1, C_2, C_3 , as illustrated in Figure 2. Moreover, we fix the segment parameters $\theta_{i,1} = \alpha/\beta = 1000$ for all time series $i \in \{1, \dots, L\}$, and $\theta_{i,2} > 1000$ for all $i \in C$. For all $i \in C$, conditional on the position of the changepoint $\tau_{i,1}$, the larger $\theta_{i,2}$ is, the stronger the signal for a changepoint is, and the level of evidence may be quantified by Monte Carlo estimation of the expected Bayes factor comparing a model with a changepoint $\tau_{i,1}$ and a model with no changepoints.

Next, we consider different graphical models of dependent changepoints, in comparison with the standard model for independent changepoints (12), to illustrate how the posterior distribution of changepoints varies with the partition C , the level of evidence for changepoints and the hyperparameters of the changepoint prior. A supplementary experiment, related to star dependence structures, is discussed in Appendix C.1.

6.1. Clusters of changepoints on a lattice and on an r -chain of time series

By considering dependence structures for changepoints that are induced by the lattice and the r -chain graphs discussed in Section 4.2, we demonstrate the merit of the graphical changepoint model to combine weak signals for changepoints across clustered time series, in comparison with the standard model for independent changepoints.

The set C is partitioned into three sets $C_1 = \{1, 2, \dots, 6\}$, $C_2 = \{17, 18, 23, 24, 29, 30\}$ and $C_3 = \{14\}$. As illustrated in Figure 2, for both the 6×5 lattice graph and the 2-chain graph, the elements of C_1 and C_2 cluster according to the graph, yet the element of C_3 has no neighbours in C so that it is isolated on the graph. For all $i \in C = C_1 \cup C_2 \cup C_3$, we set $\tau_{i,1} = 200$, so that changepoints are synchronous, and we let $\theta_{i,2} = \theta \in \{1040, 1050, 1060\}$, corresponding to increasing levels of evidence for changepoints. We performed ten simulations from each model.

The prior for synchronous dependent changepoints defined in (11) is assumed, and we consider two different dependence structures: the dependence structure corresponding to a 6×5 lattice graph for time series indices, given in Section 4.2.2; and the dependence structure corresponding

to the r -chain graph for time series indices, with $r = 2$, given in Section 4.2.3. For each simulation from the model, for each type of dependence structure for the changepoints, and for different changepoint hyperparameters $\bar{p} \in \{-60, -70, \dots, -130\}$ and $\lambda = \lambda_s |\bar{p}|/4$ with $\lambda_s \in \{0, 0.2, \dots, 0.8\}$, a sample of size 50 000 was obtained from the posterior distribution of changepoints, via the MCMC algorithm proposed in Section 5.1, with a burn-in of 10 000 iterations. We set $\delta_0 = 0.5$, $\delta_1 = 1$, $\delta_2 = 30$ for the prior of the parameter δ , so that related time series indices are expected to bond with probability 0.5 when $\delta > 0$, according to (25).

For all samples, the Monte Carlo estimates of the probabilities that $k_i = 0$ for all $i \in N$ and that $k_i < 2$ for all $i \in C$ are greater than 0.99. Figure 3 displays Monte Carlo estimates of the posterior probability that $k_i = 1$, for $i \in C_1, C_2$ and C_3 , as a function of the hyperparameters of the prior for dependent changepoints, for each dependence structure considered, and given $\theta = 1050$. As \bar{p} increases, the probability that $k_i = 1$ decreases for $i \in C = C_1 \cup C_2 \cup C_3$. For $i \in C_3$, the simulated changepoint is isolated on the graph for each dependence structure considered; therefore, the interaction parameter λ has no impact on the posterior probability that $k_i = 1$. However, for $i \in C_1 \cup C_2$, as λ increases, it becomes more likely a posteriori that $k_i = 1$, because weak signals for changepoints, relative to \bar{p} , are combined across time series which cluster according to the two graphs considered. Moreover, the posterior distribution adapts to the dependence structure for changepoints specified a priori: as λ increases, for the dependence structure induced by the 2-chain, the probability that $k_i = 1$ is greater for $i \in C_1$ than for $i \in C_2$, since the subgraph induced by C_1 has more edges than the subgraph induced by C_2 ; for the dependence structure induced by the lattice, however, the subgraph induced by C_1 has fewer edges than the subgraph induced by C_2 , so that the probability that $k_i = 1$ is smaller for $i \in C_1$ than for $i \in C_2$.

Results for other levels of evidence considered in the experiment, corresponding to $\theta \in \{1040, 1060\}$, are discussed in Appendix C.2.

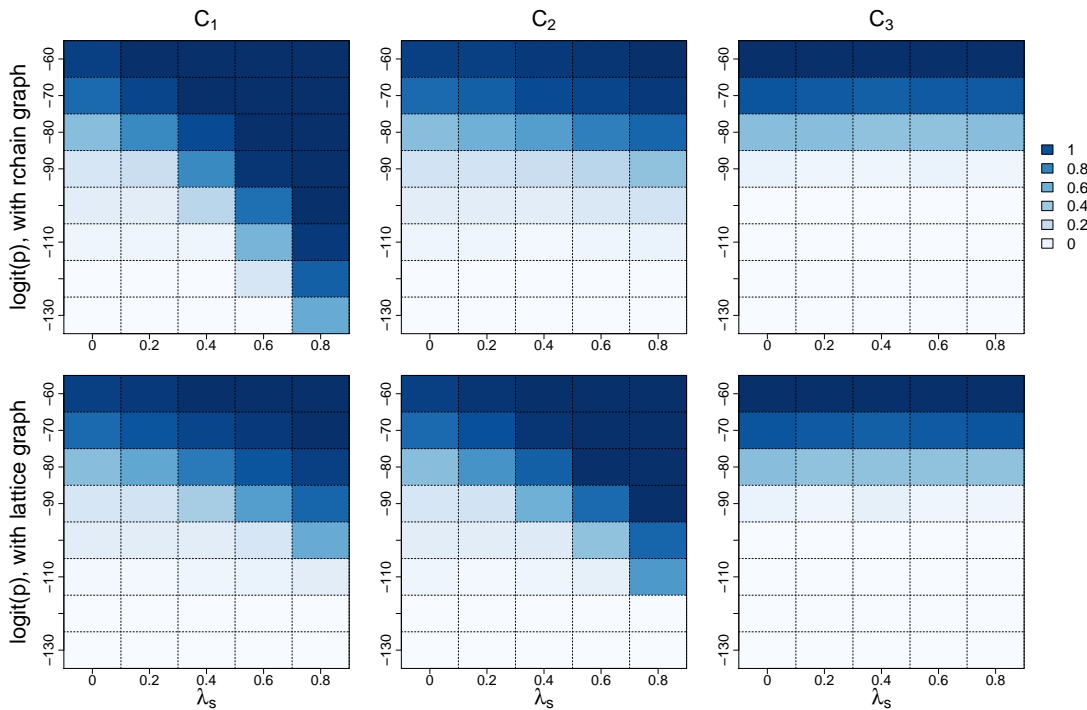


Figure 3: Monte Carlo estimates of the posterior probability that $k_i = 1$, given $\theta = 1050$, for $i \in C_1, C_2$, and C_3 , as a function of $\bar{p} = \text{logit}(p)$ and λ_s , for two types of assumed dependence structure for changepoints: 2-chain graph based dependence; lattice graph based dependence.

6.2. Importance of auxiliary variables to sample dependent changepoints

We demonstrate that it is pertinent to use auxiliary variables to sample from the posterior distribution of dependent changepoints, as discussed in Section 5. For the data generated for the experiment discussed in Section 6.1, which corresponds only to scenarios with $\theta = 1050$, changepoints were sampled via MCMC as described in Section 6.1, but now with $\delta = 0$, meaning the parameter space was not augmented with auxiliary variables. For all samples, the Monte Carlo estimates of the probabilities that $k_i = 0$ for all $i \in N$, and that $k_i < 2$ for all $i \in C = C_1 \cup C_2 \cup C_3$ is greater than 0.99. Figure 4 compares Monte Carlo estimates of the posterior probability of $k_i = 1$ from samples obtained with and without auxiliary variables, for $i \in C_1, C_2$, and for the 2-chain and the lattice graph based dependence structures for changepoints. Without auxiliary variables, the MCMC algorithm fails to explore the state space of changepoints so that the probabilities that $k_i = 1$ tend to be underestimated; in other words, clusters of weak signals for changepoints across time series tend to be overlooked. The difference in performance, in favour of the MCMC algorithm making use of auxiliary variables, is particularly important when interaction parameters are large and weak signals for changepoints correspond to time series whose indices induce subgraphs with a large number of edges, as for $i \in C_1$ given the 2-chain dependence structure in Figure 4.

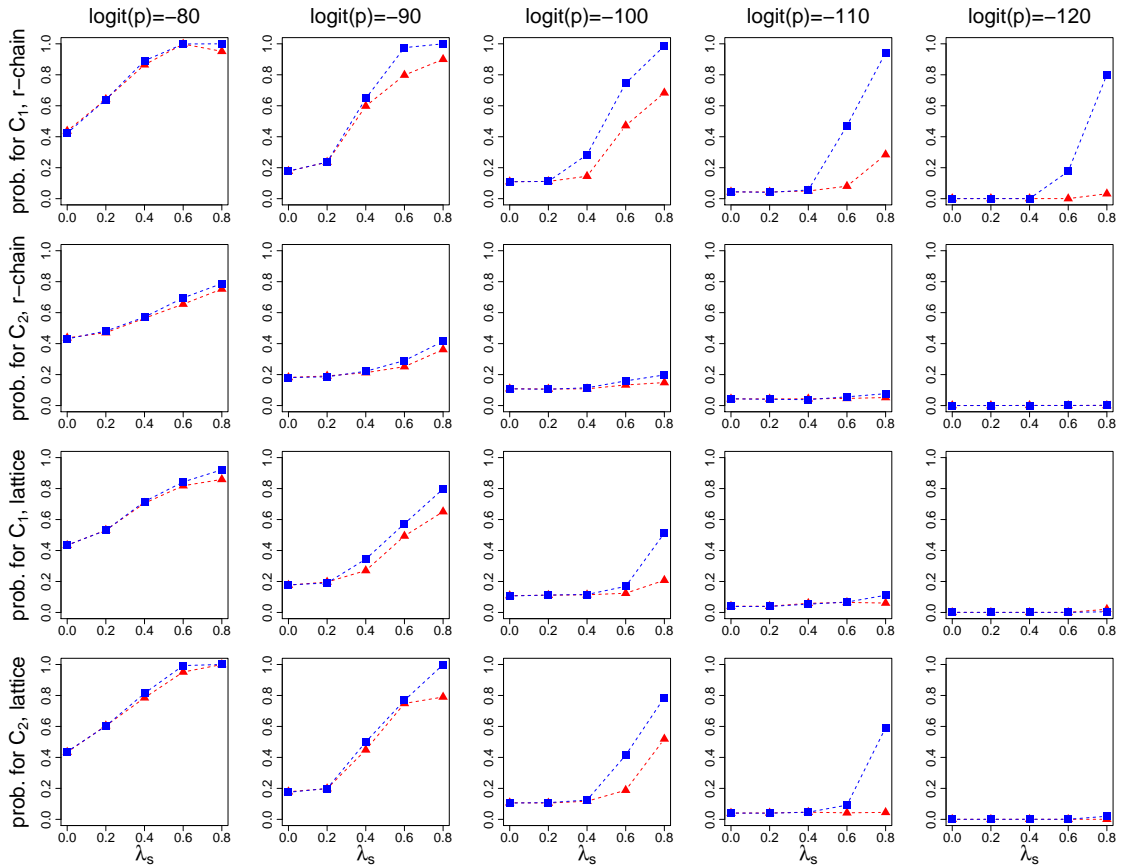


Figure 4: Monte Carlo estimates of the posterior probability that $k_i = 1$, obtained via simulations with auxiliary variables (blue squares) and without auxiliary variables (red triangles), for $i \in C_1, C_2$, for the 2-chain and the lattice graph based dependence structures, and for a collection of changepoint hyperparameters p and λ_s .

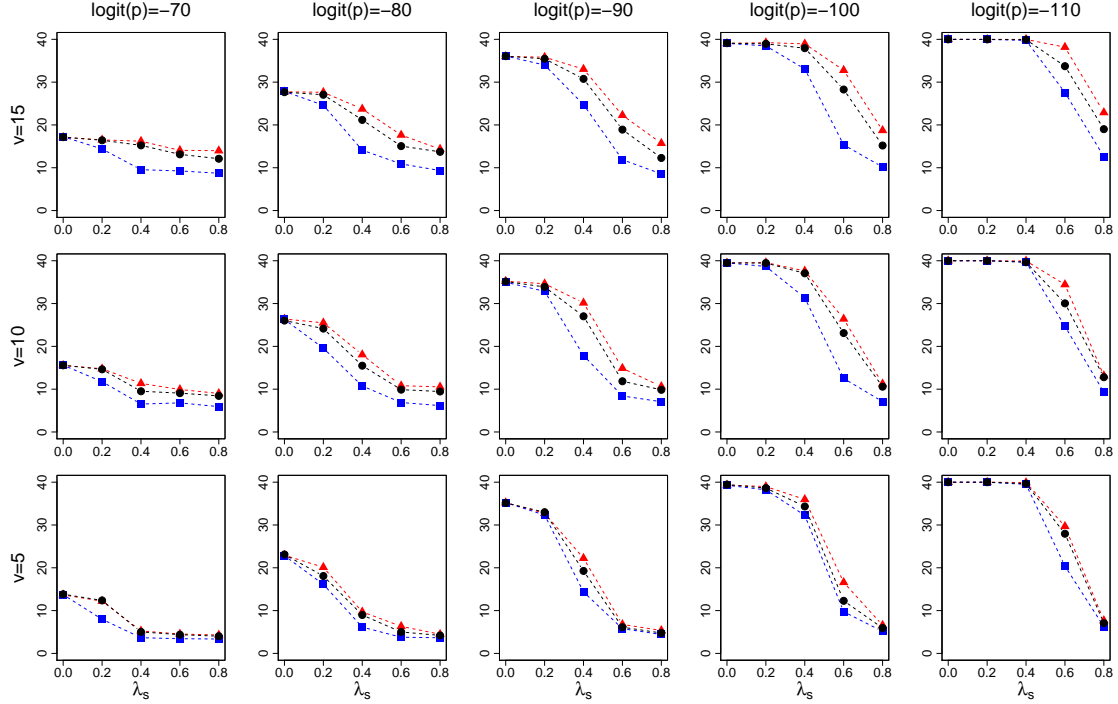


Figure 5: Monte Carlo estimates of the expected loss with respect to the simulated changepoint parameters for time series $i \in C_1$, given the 2-chain dependence structure for changepoints, corresponding to different assumptions for the upper bounds for the lags - *fixed window* (blue squares), *variable window* (black circles), and *zero window* (red triangles) - for increasing levels of asynchrony of the changepoints v , and for a collection of changepoint hyperparameters p, λ_s .

6.3. Extension to asynchronous changepoints

To illustrate the model for asynchronous dependent changepoints proposed in Section 4.3, data were simulated according to the set-up of the experiment discussed in Section 6.1, with the only difference that changepoint positions were not forced to be synchronous: for some $v > 0$, we set $\tau_{i,1} = 200 + v$ for $i \in \{3, 6, 18, 30\}$; $\tau_{i,1} = 200$ for $i \in \{2, 5, 23, 14\}$; and $\tau_{i,1} = 200 - v$ for $i \in \{1, 4, 17, 24, 29\}$, so that no two neighbouring time series, according to both the lattice graph and the 2-chain graph, are simultaneously impacted by a changepoint. For increasing levels of asynchrony for the changepoints, $v \in \{5, 10, 15\}$, ten simulations were performed from the model with $\theta = 1050$.

The prior for asynchronous dependent changepoints defined in (24) is assumed. Three different scenarios are considered for the upper bounds w for the lags: for the *fixed window* scenario, we fix $w_i = 30$ for all i ; for the *variable window* scenario, it is assumed a priori that $w_i \sim \text{Geometric}(0.9)$ for all i ; for the *zero window* scenario, we fix $w_i = 0$ for all i , which is equivalent to assuming the prior for synchronous dependent changepoints defined in (11). For each simulation from the model, for each scenario for the maximal lags, given the 2-chain dependence structure for changepoints, and for the collection of changepoint hyperparameters considered in Section 5.1, a sample of size 50 000 was obtained from the posterior distribution of changepoints, via the MCMC algorithm proposed in Section 5.2, with a burn-in of 10 000 iterations. Note that the prior for δ was specified as described in Section 6.1.

To take into account both the number and the positions of changepoints, for all scenarios considered, estimations of the posterior distribution of changepoints are compared in terms of the expected loss with respect to the changepoints that were used to sample data for the experiment, given the loss function L defined in Definition 3 with $\gamma = 40$. Figure 5 displays Monte Carlo

estimates of the expected loss for the time series in C_1 , which correspond to different assumptions for the upper bounds for the lags. As the level of asynchrony of the changepoints v increases, the expected loss tends to be greater for the *zero window* scenario than for the *fixed window* or the *variable window* scenarios. Hence, both in terms of detecting signals for changepoints and correctly estimating the positions of these signals, there is merit in relaxing the assumption that signals for changepoints must be synchronous to be combined. Moreover, the expected loss tends to be greater for the *variable window* than for the *fixed window* scenarios, therefore encouraging practitioners to specify fixed time windows when possible.

7. Red team detection in network authentication data from LANL

This section presents results of an analysis of the LANL network authentication data presented in Section 3 that demonstrates the utility of the graphical changepoint model proposed in Section 4, through a comparison with the standard model for independent changepoints across time series (4).

7.1. Presence of a red team

The occurrence of a red team exercise during the first month of the data collection provides surrogate intruder behaviour in the authentication data (Kent, 2015). In particular, 103 user IDs are known to have been used by the red team. We show the graphical model for dependent changepoints can combine evidence from multiple users which are linked in the network, to detect chains of quasi-synchronous weak signals for changes in the authentication activity of red team users, whilst limiting the number of false alerts.

For our demonstration purposes, it suffices to examine a subset of the full LANL network of users, which is represented by the graph $G = (V, E)$ defined in (9). Let R denote the set of red team users and let $N \subseteq \{u \in V \setminus R : \exists r \in R \text{ s.t. } (u, r) \in E\}$ denote $|R|$ randomly selected users that are not labelled as red team users in the data but are linked to red team users on the network. The focus is on the network corresponding to the subgraph G' induced in G by the set of users $V' = R \cup N$. Figure 6 shows the degree distribution of the 206 users in G' . Red team users tend to have a greater degree in G' than legitimate users; to traverse the network towards high value targets, intruders tend to take control of users that are highly linked on the network.

7.2. Changepoint modelling

Recall from Section 3 that, for each user $i \in V'$, the data $x_{i,1}, \dots, x_{i,T}$ consist of hourly counts of network logons per source computer for the first month of data collection as defined in (7), which are now assumed to follow the changepoint model specified in (8). To encode prior belief that signals for changes resulting from an attack are likely to occur at similar times across users that are linked in the network G' , the prior for dependent changepoints specified in (24) is assumed with an identical edge weight parameter $\lambda > 0$, as defined in Section 4.1.2, for all pairs of time series corresponding to users that are linked in G' . Recall that the same set-up with $\lambda = 0$ corresponds to the standard changepoint model assuming independence of changepoints across time series (12).

For comparison purposes and to illustrate the flexibility of the proposed model, a collection of changepoint hyperparameters are considered: $\bar{p} \in \{-40, -60, -80\}$ and $\lambda = \lambda_s |\bar{p}|/n$ with $\lambda_s \in \{0, 0.5, 0.6, 0.7, 0.8\}$, where n denotes the average node degree in G' . Moreover, different assumptions for the upper bounds w for the lags are compared: the *zero window* assumption with $w_i = 0$ for all i , implying signals for attacks are assumed to be synchronous across users; and, the *variable window* assumption with $w_i \sim \text{Geometric}(0.9)$ for all i , admitting signals for attacks may be asynchronous across users.

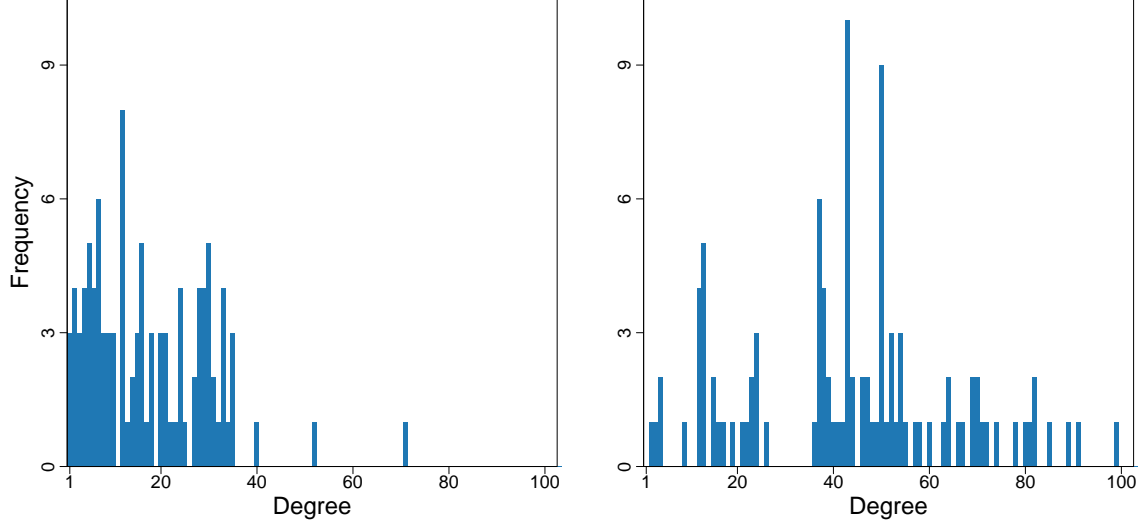


Figure 6: Degree distribution of users in the LANL network represented by the graph G' . Left panel: counts for legitimate users. Right panel: counts for red team users.

For each simulation, a sample of size 1 000 000 was obtained from the posterior distribution of the changepoints via the MCMC algorithm proposed in Section 5.2, with a burn-in of 300 000 iterations; the Bayes estimate for changepoints corresponding to the loss function (6) with $\gamma = 48$ was then derived from the sample.

7.3. Results

For each user in the network, each estimated changepoint represents a piece of evidence for possible malicious behaviour that might require further investigation by cyber analysts. Identifying inferred changepoints for time series corresponding to legitimate users $i \in N$ as false alerts, it is meaningful to compare models in terms of the estimated number of changepoints for red team users and for legitimate users. Moreover, since cyber-attacks tend to be identified through clusters of behavioural changes across machines that are linked on the network, it is of interest to prioritise for investigation the estimated changepoints that belong to clusters of quasi-synchronous changepoints on the network. Given some time window $\varpi \geq 0$, for each changepoint $\tau_{i,j}$, let

$$n_{i,j}^{\varpi} = |\{(i, i') \in E : \exists j' \in \{1, \dots, k_{i'}\} \text{ s.t. } |\tau_{i,j} - \tau_{i',j'}| \leq \varpi\}| \quad (32)$$

denote the number of users linked to user i in G' that are impacted by a changepoint within ϖ hours of $\tau_{i,j}$, and let

$$c_{i,j}^{\varpi} = \frac{n_{i,j}^{\varpi} + 1}{n_i + 1}, \quad (33)$$

where $n_i = |\{(i, i') \in E\}|$ is the degree of node i in G' , such that $(n_i + 1)^{-1} \leq c_{i,j} \leq 1$. The larger $c_{i,j}$, the more connected $\tau_{i,j}$ to other changepoints across the network. To take into account both the number of changepoints and the connectedness of the changepoints on the network, for each user i , changepoint estimates are also compared via the statistic

$$m_i \equiv m_i^{\varpi} = \sum_{j=1}^{k_i} c_{i,j}^{\varpi}, \quad (34)$$

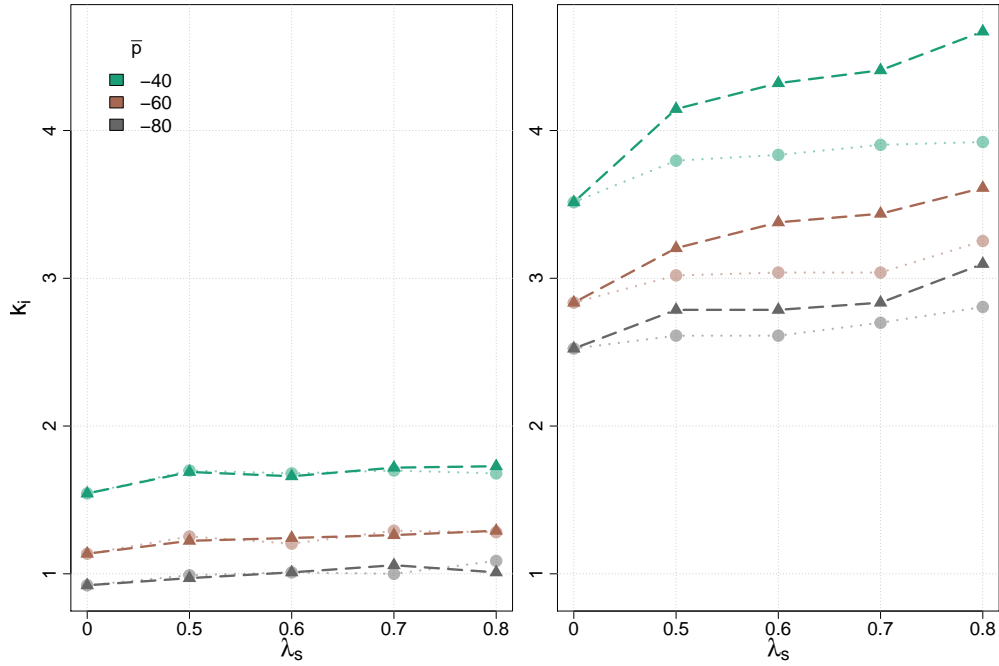


Figure 7: Estimated average number of changepoints k_i for legitimate users $i \in N$ (left panel) and for red team users $i \in R$ (right panel), for different assumptions for the upper bounds for the lags - zero window (circles) and variable window (triangles), and for a collection of hyperparameters \bar{p} (identified by distinct colours) and λ_s .

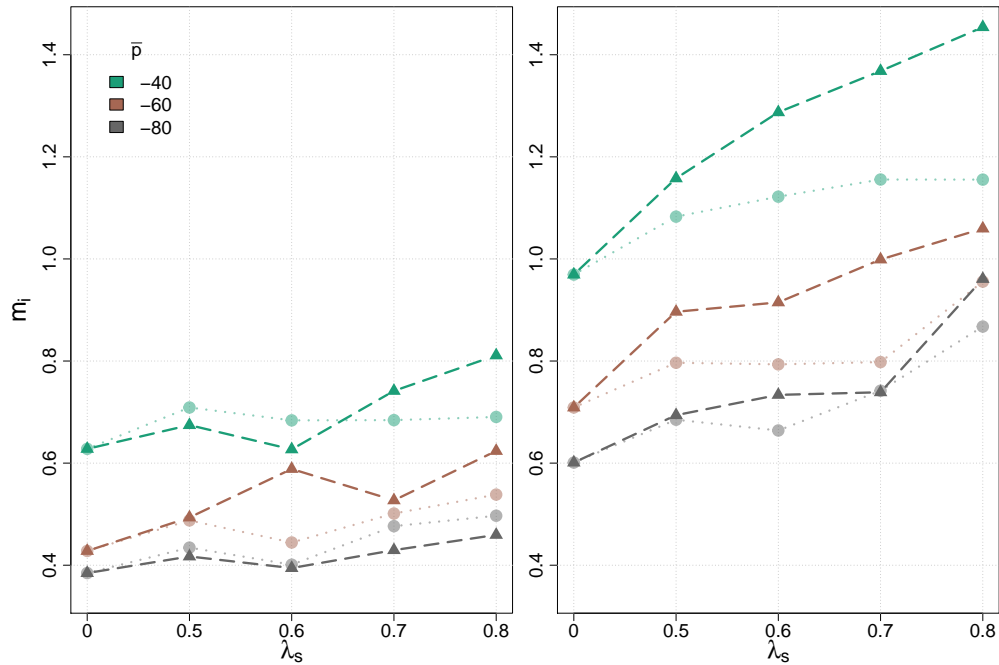


Figure 8: Estimated average m_i , as defined in (34), for legitimate users $i \in N$ (left panel) and for red team users $i \in R$ (right panel), for different assumptions for the upper bounds for the lags - zero window (circles) and variable window (triangles), and for a collection of hyperparameters \bar{p} (identified by distinct colours) and λ_s .

such that $0 \leq m_i \leq k_i$. Note that for each user i , m_i increases with both the number of changepoints and the connectedness of those changepoints.

For each choice of changepoint hyperparameters, Figure 7 and Figure 8 display the estimated average number of changepoints k_i and the estimated average m_i (34) with $\varpi = 24$, respectively, for red team users $i \in R$ and for legitimate users $i \in N$. As \bar{p} increases, weaker evidence is required to infer changepoints, and therefore the estimated values of k_i and m_i increase for both red team users and legitimate users. However, as λ increases, weaker signals are required to infer changepoints impacting multiple users that are linked on the network, and consequently the estimates for k_i and m_i tend to increase for red team users $i \in R$ only. The graphical changepoint model detects weak signals for behavioural changes that correspond to red team activity, whilst crucially limiting the number of false alerts, because it successfully encodes prior knowledge that cyber attacks tend to correspond to coordinated activity across multiple users linked by network connectivity.

Moreover, as λ increases, the increase of the estimates for k_i and m_i for red team users tends to be greater for the *variable window* scenario than for the *zero window* scenario. In contrast with the *zero window* scenario, the *variable window* scenario admits attacks may result in asynchronous behavioural changes across the network, and consequently clusters of nearby but not necessarily synchronous weak signals for changepoints are detected across red team users.

The results show that, in comparison with the standard model for independent changepoints across time series, the proposed graphical changepoint model provides a flexible tool for cyber-analysts to incorporate expert knowledge in changepoint analysis for network monitoring, thereby facilitating network intrusion detection.

8. Conclusion

This article proposes a flexible class of Bayesian changepoint models for multiple time series that is adapted to a wide range of graphical model dependence structures for changepoints across time series. A possible extension of the model is to relax the assumption that the graph G on time series indices is known a priori. It might be computationally unrealistic to specify an unconstrained prior for G . However, in some settings it might be appropriate to consider a class of possible graphs G ; for example, it may be assumed a priori that G is an r -chain, as defined in 4.2.3, with $r \geq 0$ unknown.

Supplementary material

The *python* code and the data are available at https://github.com/karl-hallgren/cp_on_graph_of_timeseries/

References

- Bardwell, L. and Fearnhead, P. (2017). Bayesian detection of abnormal segments in multiple time series. *Bayesian Analysis*, 12(1):193–218.
- Bardwell, L., Fearnhead, P., Eckley, I. A., Smith, S., and Spott, M. (2019). Most recent changepoint detection in panel data. *Technometrics*, 61(1):88–98.
- Besag, J. and Green, P. J. (1993). Spatial statistics and Bayesian computation. *Journal of the Royal Statistical Society. Series B (Methodological)*, 55(1):25–37.
- Bolton, A. D. and Heard, N. A. (2018). Malware family discovery using reversible jump MCMC sampling of regimes. *Journal of the American Statistical Association*, 113(524):1490–1502.

- Bondy, J. A. and Murty, U. S. R. (1976). *Graph Theory with Applications*. Elsevier, New York.
- Denison, D., Holmes, C., Bani, M., and Smith, A. (2002). *Bayesian Methods for Nonlinear Classification and Regression*. Wiley Series in Probability and Statistics, Chichester: Wiley.
- Fearnhead, P. (2006). Exact and efficient bayesian inference for multiple changepoint. *Statistics and Computing*, 16:203–213.
- Fisch, A., Eckley, I., and Fearnhead, P. (2019). Subset multivariate collective and point anomaly detection. *arxiv.org*.
- Green, P. J. (1995). Reversible jump Markov chain Monte Carlo computation and Bayesian model determination. *Biometrika*, 82(4):711–732.
- Grundy, T. J., Killick, R., and Mihaylov, G. (2020). High-dimensional changepoint detection via a geometrically inspired mapping. *Statistics and Computing*, 30:1155–1166.
- Higdon, D. M. (1998). Auxiliary variable methods for Markov chain Monte Carlo with applications. *Journal of the American Statistical Association*, 93(442):585–595.
- Jeng, X. J., Cai, T. T., and Li, H. (2012). Simultaneous discovery of rare and common segment variants. *Biometrika*, 100(1):157–172.
- Kent, A. D. (2015). Cybersecurity data sources for dynamic network research. In *Dynamic Networks in Cybersecurity*. Imperial College Press.
- Lauritzen, S. L. (1996). *Graphical Models*. Oxford University Press, Oxford.
- Li, F. and Zhang, N. R. (2010). Bayesian variable selection in structured high-dimensional covariate spaces with applications in genomics. *Journal of the American Statistical Association*, 105(491):1202–1214.
- Sexton, J. O., Storlie, C., and Neil, J. (2015). Attack chain detection. *Statistical Analysis and Data Mining*, 8:353–363.
- Swendsen, R. H. and Wang, J.-S. (1987). Nonuniversal critical dynamics in Monte Carlo simulations. *Phys. Rev. Lett.*, 58:86–88.
- Wang, T. and Samworth, R. J. (2018). High dimensional change point estimation via sparse projection. *Journal of the Royal Statistical Society: Series B (Statistical Methodology)*, 80(1):57–83.

Acknowledgements

The authors thank Niall Adams for stimulating discussions about this work. The authors acknowledge funding from EPSRC. Research presented in this article was supported by the Laboratory Directed Research and Development program of Los Alamos National Laboratory (New Mexico, USA) under project number 20180607ECR and Los Alamos National Laboratory.

Appendices

A. Motivational example: changepoint detection in cyber-security

This section gives further details on the motivational example discussed in Section 3.

A.1. Data processing

With the aim of modelling network activity that is human driven rather than high frequency and automated, the network authentication data, which are available online at <https://csr.lanl.gov/data/cyber1>, were filtered as follows: events involving the same pair of user and source computer more than 5 000 times were removed; computers that act as source computers for more than 300 distinct users were discarded. The resulting data involves 11 985 distinct users and 12 947 distinct source computers.

A.2. Limitations of changepoint independence across time series

To detect occurrences of malicious activity in the network, the authentication activity of each user is monitored via hourly counts of network logons per source computer. Figure 9 displays the first month of data for two distinct users that are linked on the network. The data are assumed to follow the changepoint model specified in Section 3. Assuming further that changepoints are independent with prior distribution given in (4), for a selection of Bernoulli parameters p , a sample from the posterior distribution of changepoints was obtained via the reversible jump MCMC algorithm proposed in Green (1995), adapted to discrete time changepoints. In Figure 10, for different Bernoulli parameters, the crosses and the red lines indicate the positions of Bayes changepoint estimates corresponding to the loss function L given in Definition 3 with $\gamma = 40$; it is noticeable that p controls a priori the level of granularity of the segmentation of the data. The smaller p , the stronger the evidence required from the data to suggest a posteriori inferred changes. No choice of p seems satisfactory: choosing a small value for p will limit the number of false alerts due to noise and user specific legitimate activity; yet it will also prevent the detection of weak signals for changes shared by different users which are linked in the network, that may be of great interest.

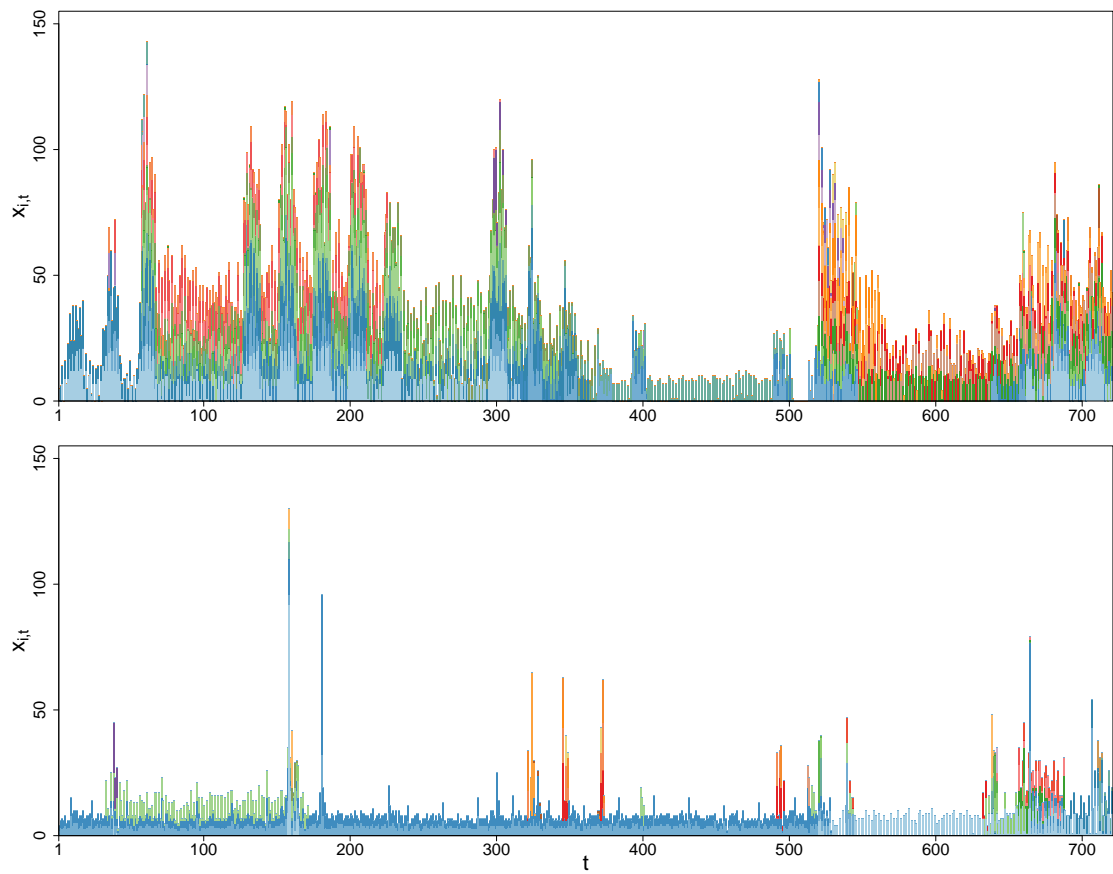


Figure 9: Hourly counts of network logons per source computer for two users over the first month of data collection. Source computers are identified by distinct colours. Top panel corresponds to user U342@DOM1, and bottom panel to user U86@DOM1.

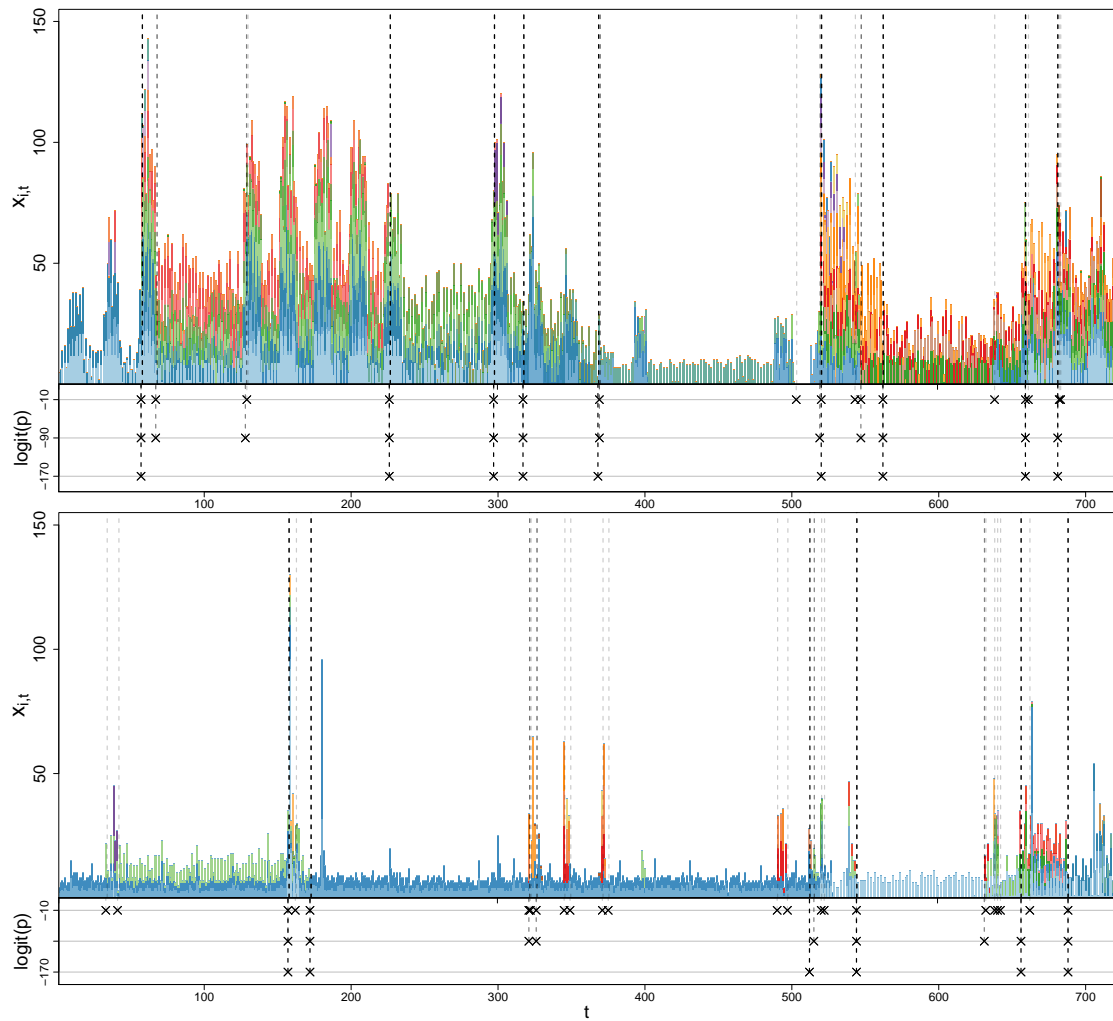


Figure 10: Hourly counts of network logons per source computer for two users over the first month of data collection; top panel corresponds to user U342@DOM1 and bottom panel to user U86@DOM1. Crosses indicate positions of Bayes changepoint estimates, according to the loss function L with $\gamma = 40$, corresponding to three different Bernoulli parameters p .

B. Proof of Proposition 1

- (i) Let $w \geq 0$, $k \geq 0$ and $\tau_{1:k} = (\tau_1, \dots, \tau_k) \in \mathcal{T}_k$. We introduce some notations to facilitate the proof. For all $0 \leq j \leq l \leq k$, let

$$\Omega_{j:l} = \Omega_{j:l}(w, k, \tau_{1:k}) = \{d_{j:l} = (d_j, \dots, d_l) : \forall i, 0 \leq d_i < \rho(i, 0) = \min\{w + 1, T + 1 - \tau_i\}\}$$

and

$$\mathcal{Q}_{j:l} \equiv \mathcal{Q}_{j:l}(w, k, \tau_{1:k}) = \{d_{j:l} = (d_j, \dots, d_l) \in \Omega_{j:l} : \tau_j + d_j \geq \tau_{j+1} + d_{j+1} \geq \dots \geq \tau_l + d_l\}.$$

Note that $|\Omega_{j:l}| = \prod_{i=j}^l \rho(i, 0)$ and $|\mathcal{Q}_{j:l}| = Q(j, l - j)$ where Q is defined in (20).

It is immediate that if $k = 0$ then (22) holds. If $k = 1$ then $|\mathcal{D}(w, k, \tau_{1:k})| = \min\{w + 1, T + 1 - \tau_1\} = Z(1)$. We show by induction that (22) holds for $k > 1$. If $k = 2$ then

$$\begin{aligned} |\mathcal{D}(w, k, \tau_{1:k})| &= |\Omega_{1:2}| - |\mathcal{Q}_{1:2}| \\ &= \rho(1, 0)\rho(2, 0) - Q(1, 1) \\ &= Z(1)Q(2, 0) - Z(0)Q(1, 1) \\ &= Z(2). \end{aligned}$$

Assume that (22) holds for $k = 1, \dots, k' - 1$ for some $k' > 2$. We show that (22) holds for $k = k'$. We have

$$\begin{aligned} |\mathcal{D}(w, k, \tau_{1:k})| &= \sum_{j=1}^k (-1)^{k-j} |\{d_{1:k} \in \Omega_{1:k} : d_{1:(j-1)} \in \mathcal{D}(w, j-1, \tau_{1:(j-1)}), d_{j:k} \in \mathcal{Q}_{j:k}\}| \\ &= \sum_{j=1}^k (-1)^{k-j} |\mathcal{D}(w, k-j, \tau_{1:(k-j)})| |\mathcal{Q}_{j:k}| \\ &= \sum_{j=1}^k (-1)^{k-j} Z(j-1)Q(j, k-j) \\ &= Z(k). \end{aligned}$$

- (ii) Follows immediately from (18).

C. Simulation study

C.1. Star of changepoints with varying number of peripheral time series affected by changepoints

Consider the dependence structure for changepoints induced by the star graph for time series indices discussed in Section 4.2.1. We demonstrate that as the number of peripheral time series affected by a changepoint at some time t increases, weaker evidence is required for the detection of a changepoint impacting the central time series $i = 1$ at time t .

As illustrated in Figure 11, the set C is partitioned into two sets C_1 and C_2 such that $C_1 = \{1\}$ contains the central time series and C_2 comprises a random subset of $\{2, \dots, L\}$ corresponding to the peripheral time series that are impacted by a changepoint. For all $i \in C = C_1 \cup C_2$, we set $\tau_{i,1} = 200$, so that changepoints are synchronous. For all peripheral time series $i \in C_2$, we fix $\theta_{i,2} = 1100$ so that the evidence for a changepoint is overwhelming relative to the hyperparameters p that will be considered for the changepoint prior. Ten simulation repetitions were performed for different numbers of peripheral time series affected by a changepoint $|C_2| \in \{0, 9, 18, 27\}$ and for different $\theta_{1,2} \in \{1040, 1050, 1060\}$ corresponding to increasing levels of evidence for a changepoint for the central time series.

The prior for synchronous dependent changepoints defined in (11) is assumed, with a parametrisation corresponding to a star graph for time series indices as discussed in Section 4.2.1. For each simulation and for different changepoint hyperparameters $\bar{p} \in \{-60, -70, \dots, -130\}$ and $\lambda = |\bar{p}|\lambda_s/(L-1)$ with $\lambda_s \in \{0, 0.2, \dots, 0.8\}$, a sample of size 50 000 was obtained from the posterior distribution of changepoints, via the MCMC algorithm proposed in Section 5.1, with a burn-in of 10 000 iterations. Recall that set-ups with $\lambda = 0$ correspond to the standard model for independent changepoints (12).

For all samples, the Monte Carlo estimates of the probabilities that $k_i = 0$ for all $i \in N$, that $k_i = 1$ with $\tau_{i,1} = 200$ for all peripheral time series $i \in C_2$, and that $k_i < 2$ for the central time series $i = 1$ are greater than 0.99. Figure 12 displays Monte Carlo estimates of the posterior probability that $k_1 = 1$ for the central time series as a function of the hyperparameters of the prior for dependent changepoints, for the different scenarios considered. It is apparent that as \bar{p} increases, stronger evidence for a changepoint is needed to infer a posteriori that the central time series is impacted by a changepoint. Moreover, if $\lambda > 0$, as the number of peripheral time series impacted by a changepoint increases, it is more likely a posteriori that the central time series is affected by a changepoint, suggesting that weaker evidence is required for the detection of a changepoint. Similarly, if $|C_2| > 0$, the posterior probability that $k_1 = 1$ increases with λ , confirming the role of the graph edge interaction parameter.

C.2. Clusters of changepoints on a lattice and on an r -chain of time series

For other levels of evidence considered in the experiment discussed in Section 6.1, corresponding to $\theta \in \{1040, 1060\}$, results are similar to results for the scenario where $\theta = 1050$. Yet, by considering results for the dependence structure corresponding to the 2-chain displayed in Figure 13, we note that, as the level of evidence increases, the region of high posterior probability that $k_i = 1$ for $i \in C$ translates along the \bar{p} axis on the \bar{p}, λ -plane.

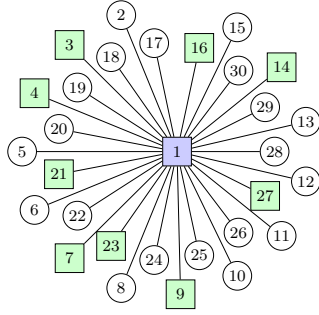


Figure 11: Exemplar graph of time series indices $i \in \{1, \dots, 30\}$ representing a star dependence structure discussed in Section 4.2. For all i , circles indicate $i \in N$ and squares indicate $i \in C$; moreover, colours blue and green indicate that $i \in C_1$ and C_2 , respectively.

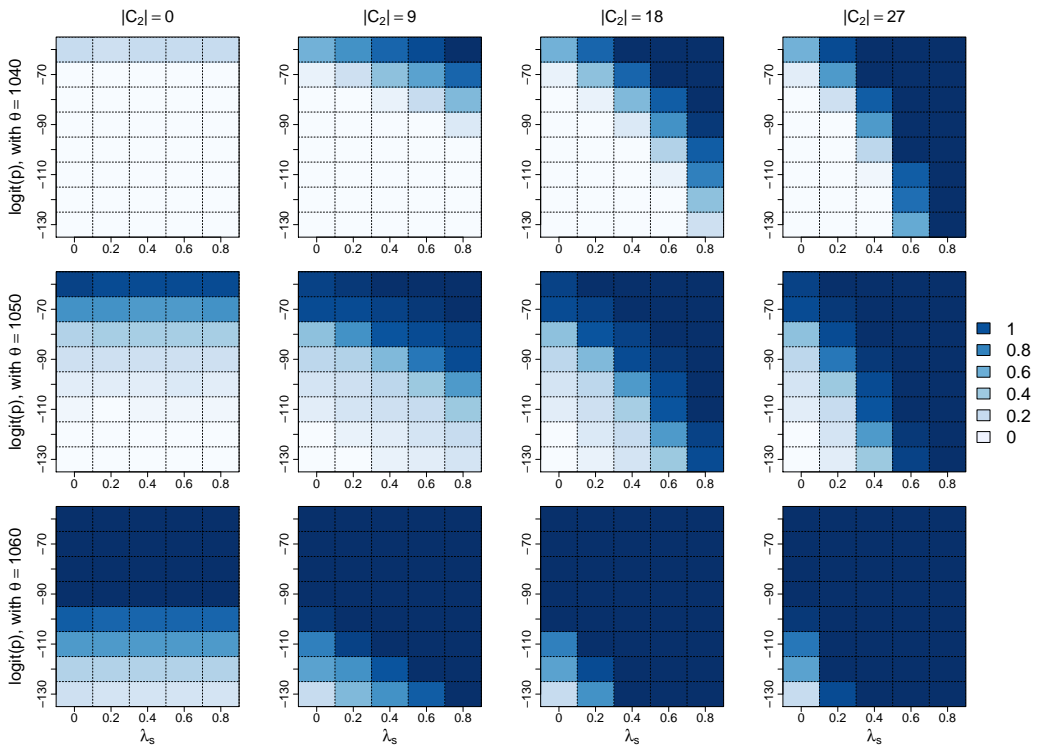


Figure 12: Monte Carlo estimates of the posterior probability that $k_i = 1$ for the central time series $i = 1$ as a function of $\bar{p} = \text{logit}(p)$ and λ_s , for different levels of evidence for a changepoint $\theta_{1,2} = \theta$ in the central series (rows) and different numbers of peripheral times series affected by a changepoint $|C_2|$ (columns).

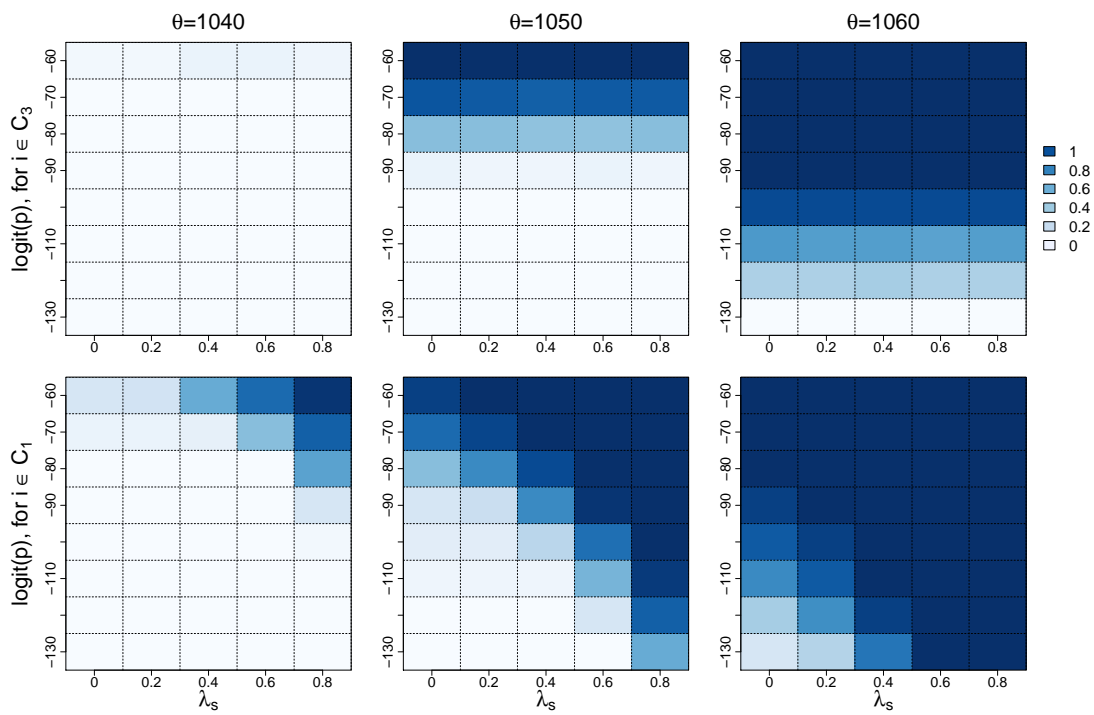


Figure 13: Monte Carlo estimates of the posterior probability that $k_i = 1$, given the 2-chain graph based dependence structure for changepoints, as a function of $\bar{p} = \text{logit}(p)$ and λ_s , for $i \in C_1, C_3$, and for different level of evidence for changepoints $\theta_{i,2} = \theta \in \{1040, 1050, 1060\}$.